A Device for Measuring Groundwater Velocity in the Capillary Fringe

by

Steven J. Berg

A thesis
presented to the University of Waterloo
in fulfillment of the
thesis requirement for the degree of
Master of Science
in
Earth Sciences

Waterloo, Ontario, Canada, 2007

AUTHOR'S DECLARATION

I hereby declare that I am the sole author of this thesis. This is a true copy of the thesis, including any required final revisions, as accepted by my examiners.

I understand that my thesis may be made electronically available to the public.

.

Abstract

Groundwater flow in the capillary fringe is rarely measured during hydrogeological studies because of the difficulties associated with investigating this region. Previous research using a point velocity probe (PVP) to investigate groundwater velocity below the water table suggested that the PVP may also be capable of measuring groundwater velocity within the capillary fringe. The earlier PVP was redesigned for this study to allow for groundwater velocity data to be collected remotely. Using this system, groundwater velocity in the capillary fringe was investigated under field and laboratory conditions. Field experiments to investigate horizontal flow in the capillary fringe were conducted either by collecting vertical velocity profiles across the water table, or by holding the probe stationary and allowing seasonal recharge to move the capillary fringe and water table past the probe. Laboratory experiments were conducted in a controlled flow tank that simulated regions of an aquifer up to 85 cm above the water table.

The redesigned PVP performed well as a remote system and provided velocity measurements up to 12 cm above the water table under field conditions. These values were consistent with those measured below the water table. In the laboratory, under conditions of drainage, groundwater velocity measurements in the capillary fringe consistent with values below the water table were measured up to 44 cm above the water table. The ability to measure horizontal flow of groundwater in the capillary fringe may open up new avenues for research in the study of contaminant transport in phreatic aquifers.

Acknowledgements

This thesis has been an invaluable learning experience, providing me with a much deeper understanding and appreciation of the scientific process. If it were not for the support, assistance, and expertise of many people it would not have been possible.

I would like to thank my supervisor Dr. Gillham for this opportunity and also for his guidance, insight and patience when trips back to the 'drawing board' were required.

I would also like to thank Andy Colclough and Krunomir Dvorski of Science Technical Services (STS) for their technical expertise and experience and Bob Ingleton for teaching me some of the field methods necessary for this project. Thanks to Aaron Vandenhoff and Eric Sykes for assisting me in the field. Thanks to Ed Cey for helping me get started with the TDR probes in the lab.

I also thank Albanie Tremblay for kindly checking up on my project during her many visits to Borden and Walid Labaky for getting me up to speed with this project.

I thank my family, Dad, Mom, and Dave for their love and support. Most importantly I thank my wife Suzanne for her unending love and support.

Dedication

To my wife Suzanne

Table of Contents

List of Tables

List of Figures

1. Introduction

1.1 Groundwater Velocity and the Capillary Fringe

For the purpose of this study, the term 'groundwater velocity' refers to both the magnitude and direction of groundwater flow.

Groundwater velocity is one of the most important, and yet, one of the most difficult hydrogeological parameters to measure reliably. An accurate knowledge of groundwater velocity is important for site characterization, predicting contaminant fate and transport, and designing and implementing effective remediation strategies. Direct methods for estimating groundwater velocity such as the Colloidal Borescope (Kearl, 1997), the Geoflow Meter® (Kerfoot, 1985) and point dilution methods use monitoring wells to access the subsurface in order to record measurements and conduct tests. Monitoring well installation methods present many opportunities for distortion of aquifer material in the vicinity of the well which may in turn result in altered local flow conditions, thus contributing to measurement error. Other possible sources of error include; filter pack selection, degree of well development, and fouling of the well over time (Lapham et al., 1997). These factors may combine to cause preferential flow either through or around a well, thus reducing the reliability of groundwater velocity measurements taken inside a well.

For the purpose of this paper, the definitions relating to the different groundwater flow regimes are based on Xie (1994). See Figure 1.1. The *saturated zone* is 100% saturated (acknowledging the presence of possible entrapped air due to water table fluctuations) and is located immediately below the water table. The *capillary fringe* is the zone immediately above the water table that remains at or near saturation. The *transition zone* is the zone above the capillary fringe where saturation values drop from 100% to residual saturation. Collectively, the capillary fringe and transition zone are referred to as the *interface zone* (i.e. the interface between residually saturated media and the water table). Above the interface zone is the *residual saturation zone*. In this thesis, the main areas of interest are the saturated zone and the capillary fringe.

The occurrence of lateral flow in the capillary fringe has long been observed based on several laboratory experiments (Wyckoff et al., 1932; and Luthin and Day, 1955). More recently, it has been suggested that the capillary fringe may play an important role in the transport of shallow aquifer contaminants (Xie, 1994; Silliman et al., 2002; and Berkowitz et al., 2004). Despite this, groundwater flow and contaminant transport in the capillary fringe is rarely accounted for during traditional groundwater investigations. This is because the capillary fringe is not observed in monitoring wells, and thus, is often excluded from these studies.

Since it is not possible to observe water from the capillary fringe in monitoring wells, it is also not possible to measure groundwater flow within the capillary fringe using direct methods that require a well. Thus, a device capable of measuring groundwater velocity both below the water table and within the capillary fringe, without the errors associated with monitoring wells, could be very useful.

1.2 Background to this Study

To avoid the potential error caused by the installation of monitoring wells, an in situ groundwater velocity probe that does not rely on the presence of a monitoring well has been developed (Di Biase, 1999; Donald, 2001; and Labaky, 2004). The Point Velocity Probe (PVP) is an in situ device that was initially proposed by Devlin (2004). The PVP operates on the principles of Ideal Flow Theory which describes fluid flow around an object (discussed in more detail in section 2.1). The PVP is installed in direct contact with the soil; thus, it is able to measure groundwater flow both below the water table and within the capillary fringe, while avoiding the errors associated with monitoring wells. Initial laboratory research into the concept (Di Biase, 1999) produced promising results which led to rigorous error analysis and field experiments conducted by Labaky (2004). Labaky (2004) also compared measurements made with the PVP to other devices for measuring groundwater velocity: the Geoflow® Meter (Kerfoot, 1985), Point Dilution, and the Colloidal Borescope (Kearl, 1997). Of these methods, Labaky (2004) found the PVP to be the most accurate when measured velocity values were compared to expected values based on controlled flow experiments under field conditions.

More recently, the PVP concept has been applied to a permanent probe installation to investigate changes in groundwater velocity in a controlled gasoline plume (McGlashan et al., 2006). This investigation included 20 PVP's installed in an array perpendicular to groundwater flow.

1.3 Goals and Objectives

Under laboratory conditions, Labaky (2004) demonstrated the ability of the probe to measure lateral groundwater velocity within the lower portions of the capillary fringe (up to 5 cm above the water table). The measured velocities were consistent with those below the water table. These results were promising and were the motivation for this thesis.

1.3.1 Goals

The following two goals of this study were designed to address several of the recommendations made by Labaky (2004):

1) to redesign the previous PVP to increase its operational efficiency and improve user friendliness; and
2) to demonstrate the ability of the redesigned probe to measure groundwater velocity within the capillary fringe.

1.3.2 Objectives

In order for the goals listed in section 1.3.1 to be realized, several objectives needed to be met:

1) simplify the operation of the PVP;
2) increase the reliability and reproducibility of groundwater velocity readings;
3) adapt the system to be operated remotely;
4) conduct controlled field experiments to demonstrate the probes ability to measure groundwater velocity in the capillary fringe; and

5) conduct laboratory research to better understand the ability of the probe to measure groundwater velocity within the capillary fringe.

This thesis is organized into 6 chapters.

Chapter 2 presents capillary fringe theory and ideal flow theory.

Chapter 3 outlines the design changes made to the probe.

Chapter 4 describes the results from controlled field experiments.

Chapter 5 presents the results from controlled laboratory experiments designed to evaluate PVP performance within the capillary fringe.

Chapter 6 states the conclusions from these experiments and provides recommendations for future research and use of the probe.

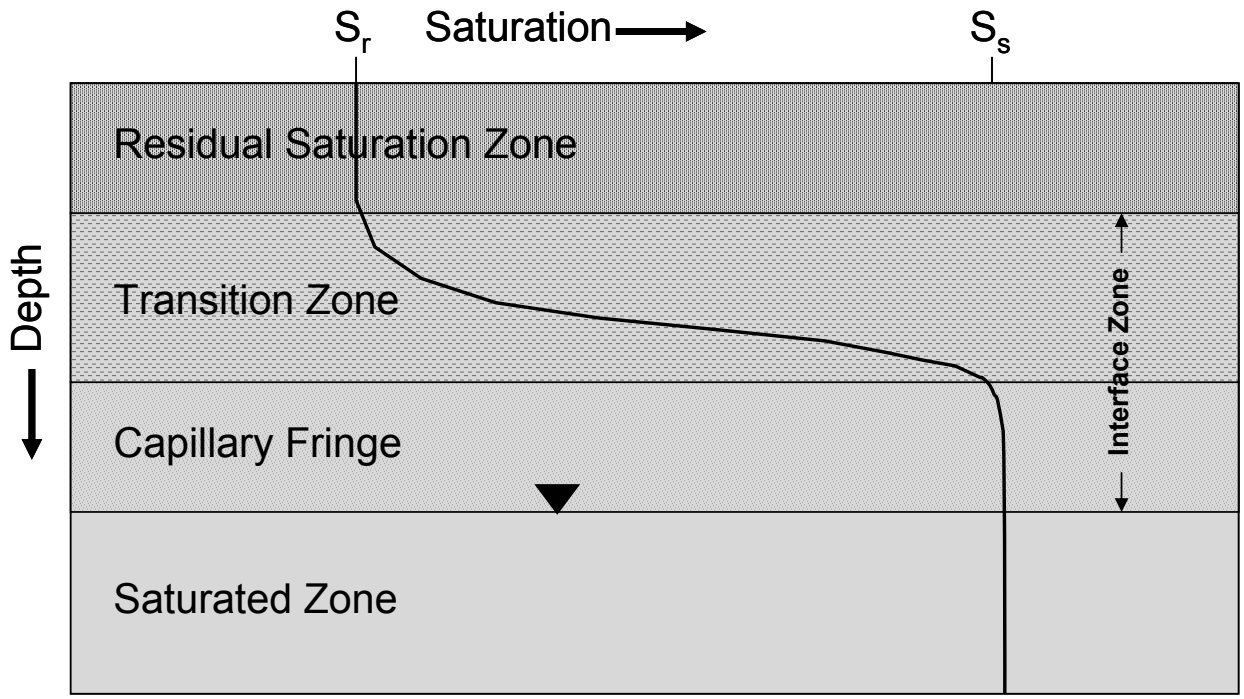

Figure 1.1 Conceptual model of the interface zone, after Xie (1994).

2. Theory

2.1 Ideal Flow Theory

Measurement of groundwater velocity with the PVP is based on the theory of ideal flow around a circular cylinder (Figure 2.1). Applying Ideal Flow Theory, as described in Bird et al. (2002), the x- and y- components of the velocity at any point in a fluid flowing around a cylinder can be calculated by:

$$v_x = v_\infty \left(1 - \frac{R^2}{r^2} \cos 2\theta \right) \quad [1]$$

$$v_y = -v_\infty \left(\frac{R^2}{r^2} \sin 2\theta \right) \quad [2]$$

where

v_∞ = the velocity of the fluid that is undisturbed by the presence of the probe, referred to as the 'approach velocity' [L/T];

R = the radius of the circular cylinder [L];

r = the distance to the point of investigation from the center of the probe [L]; and

θ = the angle between the flow direction of v_∞ and the measurement location relative to the center of the probe [degrees].

Simplifying for the case where the investigation distance *r*, is the surface of the probe *R* (i.e. $r = R$), the equation simplifies to (Bird et al., 2002):

$$v^2 = v_x^2 + v_y^2 \quad [3]$$

$$v^2 = v_\infty^2\left[(1-\cos 2\theta)^2 + (\sin 2\theta)^2\right] \quad [4]$$

$$v^2 = 4v_\infty^2 \sin^2\theta \quad [5]$$

$$|v(\theta)| = 2v_\infty \sin\ \theta \quad [6]$$

where $|v(\theta)|$ is the instantaneous velocity of the fluid on the surface of the probe at location θ.

By integrating $|v(\theta)|$ over an arc interval γ_1 or γ_2 as shown in Figure 2.2, Labaky (2004) developed equation [7] to calculate the approach velocity (v_∞):

$$v_\infty = \frac{v_{apparent} \times \gamma}{2(\cos\alpha - \cos(\alpha+\gamma))} \quad [7]$$

where

v_∞ = the approach velocity [L/T];

$v_{apparent}$ = the apparent velocity measured on the surface of the probe [L/T];

α = the angle between the point of tracer injection and the background fluid flow direction [degrees];

γ = the angle between the injection point and the detector [degrees].

It should be noted that γ is fixed during the construction of the probe and alpha (α) varies depending on the orientation of the probe with respect to the flow direction.

Taking advantage of this theory, a probe can be constructed that consists of an injection port which releases a tracer and sensors that detect the passing of this tracer (Figure 2.2). Measurement of the time of arrival of the tracer at the sensors is used to determine $v_{apparent}$.

It is important to note that the points on the surface of the probe where $\theta = 0°$ and $\theta = 180°$ are referred to as 'stagnation points'. At these points no flow occurs and thus, for practical

reasons, it is important to avoid installing the probe with the injection port at either of these locations.

If the orientation of the probe relative to the groundwater flow direction (α) is known, then the approach velocity (v_∞) can be calculated directly from equation [7] since γ is fixed during probe construction (Labaky, 2004). If the orientation of the probe relative to the groundwater flow direction is not known, it is possible to calculate the orientation by measuring the apparent velocity ($v_{apparent}$) on two different sensors. Since both sensors should produce the same approach velocity (v_∞), it is possible to equate the apparent velocities ($v_{apparent1}$ and $v_{apparent2}$) through the approach velocity (v_∞) and solve for α (Labaky, 2004):

$$\frac{v_{apparent1} \times \gamma_1}{(\cos\alpha - \cos(\alpha + \gamma_1))} = \frac{v_{apparent2} \times \gamma_2}{(\cos\alpha - \cos(\alpha + \gamma_2))} \quad [8]$$

This simplifies to (Labaky, 2004)

$$\alpha = \tan^{-1}\left[\frac{v_{apparent1}\gamma_1(\cos\gamma_2 - 1) + v_{apparent2}\gamma_2(1 - \cos\gamma_1)}{v_{apparent1}\gamma_1 \sin\gamma_2 - v_{apparent2}\gamma_2 \sin\gamma_1}\right] \quad [9]$$

By applying equations [7] and [9] to a cylindrical probe in direct contact with soil, it is possible to measure groundwater velocity (magnitude and direction) by injecting a tracer solution at a fixed position on the surface of a probe and monitoring the time of appearance at a down-gradient point on the surface of the probe. The tracer used to measure groundwater velocity was selected by Di Biase (1999) based on the following criteria:

1) ability to travel at the same velocity as the groundwater (i.e., conservative);
2) have low to non-detectable background concentrations;
3) is environmentally safe; and
4) is inexpensive and readily available.

Based on these criteria, Di Biase (1999) selected sodium chloride solution (NaCl). This selection is also advantageous for this study because inorganic salts have a minimal effect on surface tension (Davies and Rideal, 1963) and sodium chloride solution is electrically

conductive. In comparison, some organic compounds have been shown to have a profound effect on surface tension (Smith and Gillham, 1994; and Smith and Gillham, 1999). When conducting experiments in the capillary fringe, it is important that the tracer has a minimal effect on the surface tension of water and soil since a change in surface tension may affect both flow in the capillary fringe and the capillary fringe thickness. In addition to altering capillary fringe thickness, it is also possible to induce local flow by altering the surface tension (Henry and Smith, 2003).

Labaky (2004) used a 600 mg/L $NaCl_{(aq)}$ solution for laboratory experiments; however, due to the high background electrical conductivity of the groundwater at C.F.B. Borden, it was necessary to increase the tracer concentration to 6000 mg/L. This solution concentration was used for the experiments in this thesis. The tracer is detected by measuring changes in electrical conductivity (the ability of the fluid flowing around the probe to conduct an electrical current) on the surface of the probe as the tracer moves past sensors. Figure 2.3 shows typical breakthrough curves generated as the NaCl solution pulse flows past a set of two sensors. The first peak corresponds to the tracer passing the sensor closest to the injection port, while the second peak corresponds to the same tracer pulse moving past the second sensor. The second peak is wider and of lower magnitude due to the additional dispersion and diffusion experienced resulting from the longer flow path relative to the first sensor. These breakthrough curves are interpreted using PULSEPE (Devlin, 1994) to determine the apparent velocity ($v_{apparent}$) between the injection port and the sensor at which the pulse was measured. PULSEPE is a parameter estimation program that compares theoretical velocity curves to the recorded data until the match with the least error is obtained (Devlin, 1994).

2.2 Capillary Fringe Flow Theory

Most research in the field of hydrogeology focuses on flow and transport in the saturated zone below the water table. In most cases, under saturated conditions below the water table, groundwater flow can be represented by Darcy's Law. That is, the rate at which groundwater flows is directly proportional to the hydraulic gradient (i), with the constant of proportionality being the hydraulic conductivity (K). This can be expressed by equation [10] (Fetter, 2001):

$$q = -Ki \qquad [10]$$

where

q = specific discharge (volume discharge of water per unit area of soil) [L/T];

K = hydraulic conductivity [L/T]; and

i = hydraulic gradient (change in hydraulic head per unit distance) [ ].

Specific discharge (q) is related to the average linear velocity (v) through a porous medium by [11]:

$$v = \frac{q}{n} \qquad [11]$$

where:

v = average linear velocity [L/T]; and

n = porosity [ ].

Less research has been given to flow processes that exist within the capillary fringe. Water within the capillary fringe is under negative pressure relative to atmospheric pressure. The height to which the top of the capillary fringe rises above the water table is dependent on the radius of the pore throats between soil grains. Capillary fringe thicknesses can range from less than a centimeter in coarse grained material to over ten meters in fine grained materials such as clays (Bear, 1972; Gillham, 1984). For a capillary tube, the relation between pore size (radius) and the height of water rise is expressed by [12]:

$$h = \frac{2\sigma \cos\theta}{\rho g r} \qquad [12]$$

where

h = the height of rise due to capillary action [L];

σ = the interfacial tension of the fluid [M/T^2];

θ = the angle of contact between the fluid and the capillary tube [degrees];

ρ = the density of the fluid [M/L^3];

g = the acceleration due to gravity [L/T^2]; and

r = the radius of the capillary tube [L].

The connected pores between individual grains in a soil are often represented as a capillary tube. These pores are responsible for generating the tension (negative pressure) necessary to produce the capillary fringe. Since all of the pores in a soil are not the same size, drainage of different pores occurs at different tensions (different heights above the water table). It is this range in pore sizes that determines the thickness of the transition zone (the zone where saturation ranges from 100% to residual) and the shape of the water content profile.

As saturation decreases with increasing height above the water table, the largest pores drain first. Since flow through a pore (Q) is proportional to the fourth power of the radius of the pore (R^4) there is a significant decrease in flow as the largest pores begin to drain (Bird et al., 2002). Thus, if the radius of a pore were reduced by half, the resulting flow through the pore would be $1/16^{th}$ the original. Therefore, as the largest pores drain, there is a significant reduction in hydraulic conductivity of a porous medium denoted by $K(\theta)$ or $K(\psi)$. Several mathematical expressions are available to represent this relationship (e.g., Brooks and Corey, 1964; Mualem, 1976; and van Genuchten, 1980). As the hydraulic conductivity decreases, the flux (q) through the soil also decreases. In response to a decrease in saturation, the amount of water flowing through the soil decreases rapidly.

The significance of fluid transport in the capillary fringe has been recognized since at least 1932 (Wyckoff et al., 1932) when radial flow to a well was investigated under laboratory

conditions. However, measuring flow in the capillary fringe under field conditions is difficult because water present in the capillary fringe is under negative pressure head (relative to atmospheric) and will therefore not flow into a well screen (zero pressure head, or atmospheric). Thus, it is not possible to measure groundwater flow in the capillary fringe using methods that rely on monitoring wells.

Modelling results (Xie, 1994) and laboratory experiments (Wyckoff et al., 1932; Silliman et al., 2002; Labaky, 2004; and Berkowitz et al., 2004) suggest that under non-recharge conditions, horizontal flow similar in magnitude and direction to that which occurs below the water table might also be expected in the capillary fringe. This is supported by preliminary laboratory investigations by Labaky (2004) which demonstrated that flow in the lower portion of the capillary fringe (5 cm above the water table) is consistent with flow below the water table.

Recharge and water table fluctuations have been shown to potentially lead to the entrapment of air in the upper portions of shallow phreatic aquifers (Ronen et al., 1989; Ryan et al., 2000; and Dunn and Silliman, 2003). The presence of this trapped air is suspected to reduce the hydraulic conductivity of the affected soil. The zone in which the hydraulic conductivity is reduced is referred to as the ‘stagnant flow zone’. This zone extends to a theoretical maximum of approximately 1 m below the top of the saturated zone (Ronen et al., 1989). Measuring groundwater velocity with a PVP in this zone may lead to a better understanding of this phenomenon.

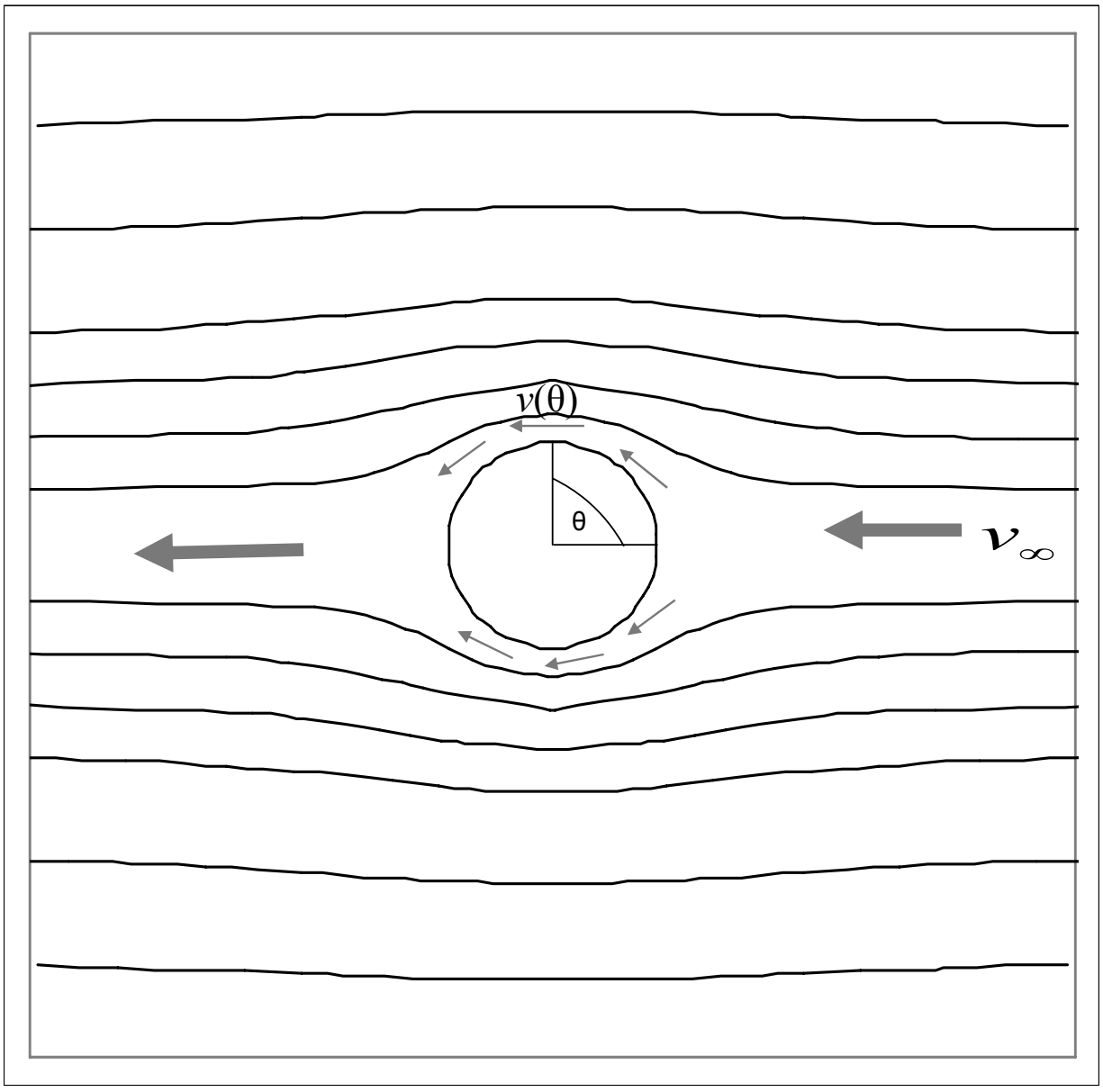

Figure 2.1 Flow around a circular cylinder as described by the Ideal Flow Theory, after Bird et al. (2002) and Labaky (2004).

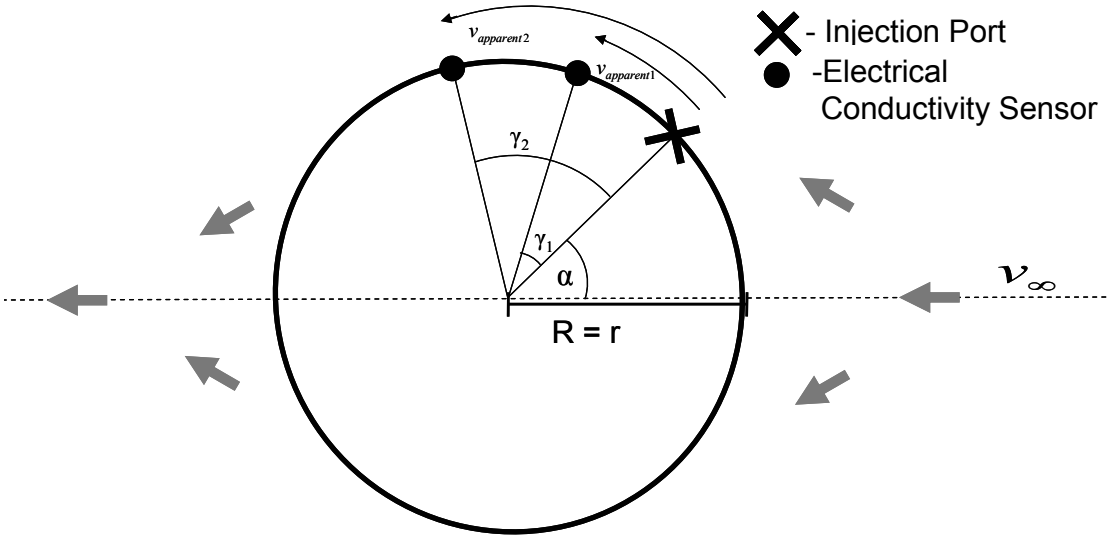

Figure 2.2 Conceptual diagram of the PVP, after Labaky (2004).

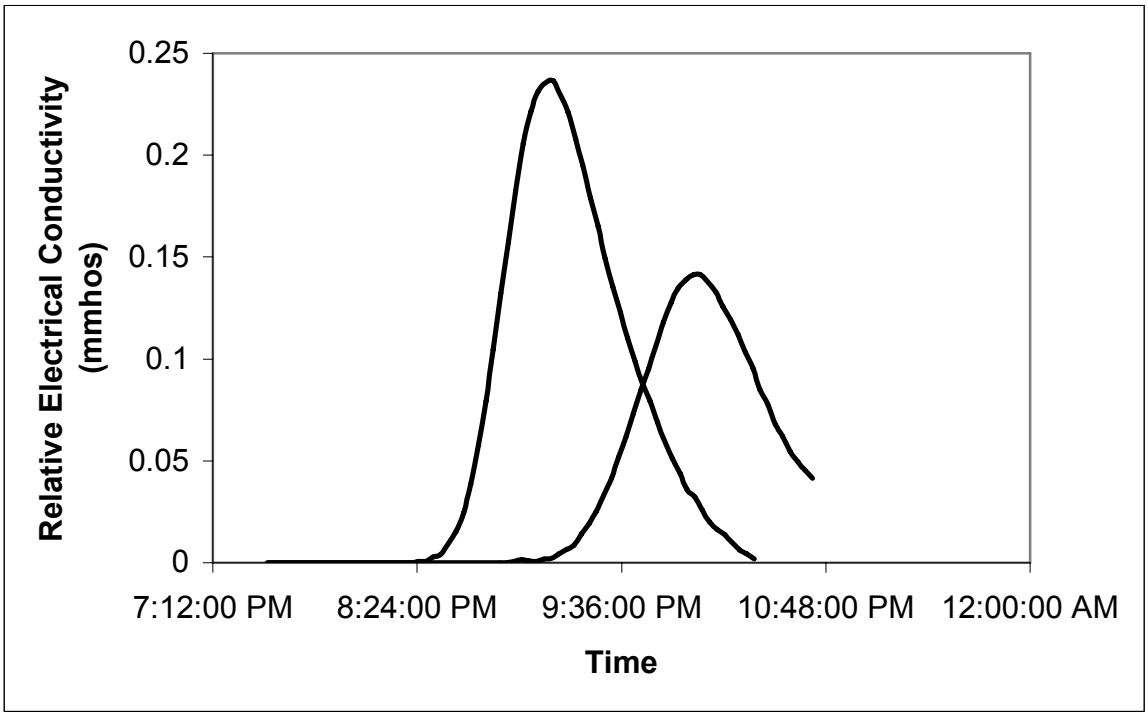

Figure 2.3 Typical breakthrough curves (Relative Electrical Conductivity vs. Time).

3. Design Changes and Improvements

In order to prepare the probe for the field study, several design changes were made. The design for the new PVP was adapted from that used by Labaky (2004) with a focus on improving performance and modifying the PVP to be operated remotely. In order to meet these goals, the objectives listed below were addressed:

1) develop an injection method that produces precise and reproducible injections;
2) redesign the probe such that measurements can be made independent of orientation to flow direction;
3) develop a data collection system that can monitor all sensors while maintaining adequate data density for analysis;
4) design a computer-controlled system for moving the probe vertically, allowing for a vertical profile of groundwater velocity to be collected; and
5) adapt the entire system to be computer controlled, thus allowing for the entire system to be remotely operated over the internet.

For the remainder of this chapter, any references to the 'previous design' or 'previous PVP' refer to the model constructed and used by Labaky (2004).

3.1 Probe Overview

In order to house the equipment for the following design changes, it was necessary to increase the diameter of the probe to approximately 4.5 cm (1.75") from approximately 3.4 cm (1.32") as used in the previous design. The probe was constructed from an approximately 90 cm long piece of 4.5 cm diameter (1.75") PVC rod. The PVC rod was split into two halves and hollowed, thus creating space for the injection system and wiring. A 1.6 mm (1/16") thick piece of rubber was placed between the two halves to create a seal when closed.

Figure 3.1 is an overview of the probe with the location of the sensors and injection ports indicated. Figure 3.2 is a picture of the interior of the probe. The remainder of this chapter will discuss the major design changes.

3.2 Sensor and Injection Port Configuration

In order for groundwater velocity to be measured by the probe, an injection port must be oriented to the groundwater flow, avoiding $\theta = 0°$ and $\theta = 180°$. This allows for the injected tracer to be carried past the electrical conductivity sensors by groundwater flow. The previous design consisted of one injection port with two electrical conductivity sensors located on either side of the injection port. Use of this design either required prior knowledge of the groundwater flow direction, or required the user to turn the probe once realizing that it was not oriented with the flow. See Figure 3.3 for an illustration of this situation.

In order to avoid requiring prior knowledge of the groundwater flow direction, the number of injection ports was increased to three, located symmetrically around the perimeter of the probe (Figure 3.4). Each injection port was accompanied by a pair of sensors located at 30° and 60° (approximately 1.2 cm and 2.4 cm respectively) from the injection port. The additional injection ports add redundancy to the system by allowing the tracer pulses to be detected at additional sensors. This allows for the possibility of simultaneously recording two groundwater velocity readings at the same elevation (one on each side of the probe). An example of the data collected using the new probe which illustrates this redundancy can be seen in Figure 3.5. During the collection of these data, the probe was installed in the orientation shown in Figure 3.4. The first two peaks in Figure 3.5 correspond to the injection released from the injection port located near the top of the figure. The third and fourth peaks correspond to the injection released from the injection port located on the bottom right side of the figure.

Additional electrical conductivity sensors were installed 5, 9, and 13 cm above the level of the injection ports (Figure 3.6). These sensors allow the operator to take a snapshot of electrical conductivity at these discrete intervals above the location at which groundwater velocity is measured. These values give the operator a sense of whether or not the area above the probes main sensors are in contact with the surrounding geological material, thus allowing the operator to make an informed decision concerning the level at which the next readings should be taken.

The electrical conductivity values presented in Figure 3.5 are relative values in that the background electrical conductivity was subtracted from the measured values. Also, it is not

possible to measure the absolute electrical conductivity values with these sensors due to their arbitrary construction; thus, it is the change in the measured value that is important.

Each electrical conductivity sensor was constructed from two pieces of copper wire which were installed flush with the surface of the probe (see Figure 3.7). These wires were then connected to a cable on the inside of the probe that ran through the drill rods to surface where they were connected to a sensor switching unit controlled by a data acquisition board (DAQ).

3.3 Injection Method

The previous injection method required the operator to use a graduated roller clamp connected to the end of a polyethylene injection line which ran down the inside of the drill rods to an injection port on the surface of the probe. Since the desired injection volume was approximately 10 µl, it was often difficult for the operator to accurately control the injection.

The injection method was modified with the goals of eliminating the need for an on-site operator, as well as increasing the accuracy and reproducibility of the injections. A Nema 8 Stepper Motor was connected to three 500 µl Hamilton syringes by use of a 'rotational to linear motion converter'. The motor, when operated by a computer, injected a preset volume (10 µl in most cases) from all three syringes. For every 1.5 revolutions of the motor, 10 µl of 6000 mg/L NaCl solution was injected. Each syringe was connected to one of the injection ports located on the surface of the probe. The injection ports on the surface of the probe were constructed by inserting a piece of 0.3 mm ID tubing inside a 0.8 mm ID tubing. If the inner tube was blocked by a sand grain this configuration allowed the injection to occur from the annulus between the two tubes. This allows for the diameter of the injection to still remain small while decreasing the chance of the injection being blocked. Figure 3.7 shows a close-up image of an injection port and associated electrical conductivity sensors.

These modifications allow for reproducible injections; however, due to the limited volume of the syringes, a maximum of approximately 42 injections are available when 10 µl injections are used. After the syringes are empty, the probe is withdrawn from the aquifer and the syringes are refilled. The syringes were filled with the tracer solution by immersing the probe

in a container holding the solution. The motor was then run in reverse, causing the syringes to fill.

3.4 Data Collection

With the previous PVP design, electrical interference between adjacent electrical conductivity sensors made it necessary to perform two injections in order to obtain one groundwater velocity value. The first tracer injection was monitored at the sensor furthest from the injection port. Once this pulse was recorded, the injection was repeated and monitored at the sensor closest to the injection port. This greatly increased the amount of time required to collect data, decreasing the practicality of the instrument, particularly in slow moving groundwater regimes.

Modifying the probe so that only one injection was required to measure groundwater velocity was critical when considering the fact that the new design has a limited number of injections possible due to the fact that the syringes are housed within the probe and can only be filled by removing the probe. To prevent interference, the sensors were monitored sequentially one at a time. Since only one sensor is monitored at a time, the possibility of electrical interference between sensors is eliminated; and it is possible to collect groundwater velocity data with only one injection. During the course of the experiments, up to eight sensors were monitored in this manner.

3.5 Vertical Profile Control (Probe Movement)

Collection of vertical velocity profiles with the previous design required an operator to manually jack the probe to the next desired elevation. This was repeated every time a velocity measurement at a new level was to be recorded.

In order to meet the remote operation objective of this thesis, probe movement needed to be performed by an electronic device. A 1500lb DC winch was connected to a drill rod connected to the probe. See Figure 3.8 for a picture of the setup of the winch and probe in the field. The winch was started by the computer and raised the probe until a magnet attached to the collar on the winch passed a stationary magnetic reed switch which then stopped the operation of the

winch. The probe could be raised in 2.5 or 5 cm intervals depending on how the winch was connected.

3.6 Remote Operation of the Probe

All of the design changes listed in this chapter were made with the intent of satisfying the remote operation objective. Thus, the injections, data collection, and probe movement were all controlled by a computer. The on-site computer was connected to the internet and using remote desktop software, the entire system was controlled remotely. This significantly reduces the operating costs as it allows the user to operate the system almost continuously, increasing productivity. To monitor the site and insure that the winch was operated safely, a web cam was attached to the system.

Operation of all components of this system (injections, data collection, and probe movement) was controlled by a program written specifically for this purpose. Figure 3.9 shows a flow chart of system operation.

Figure 3.1 Overview picture of the redesigned PVP with location of sensors and injection ports indicated.

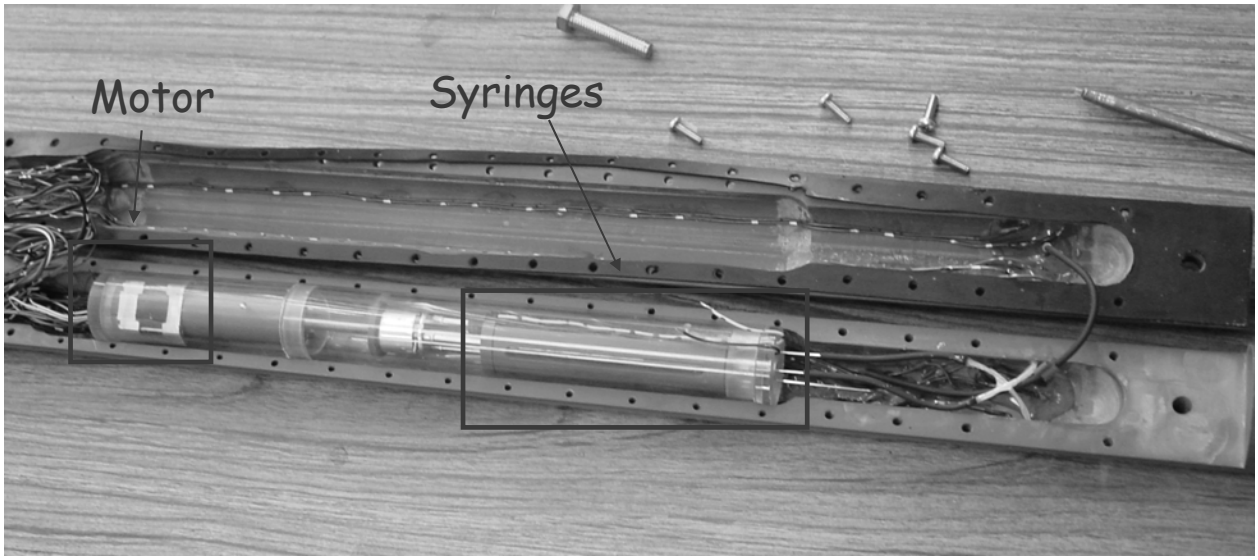

Figure 3.2 Internal picture of PVP with location of Nema 8 Stepper Motor and syringes indicated.

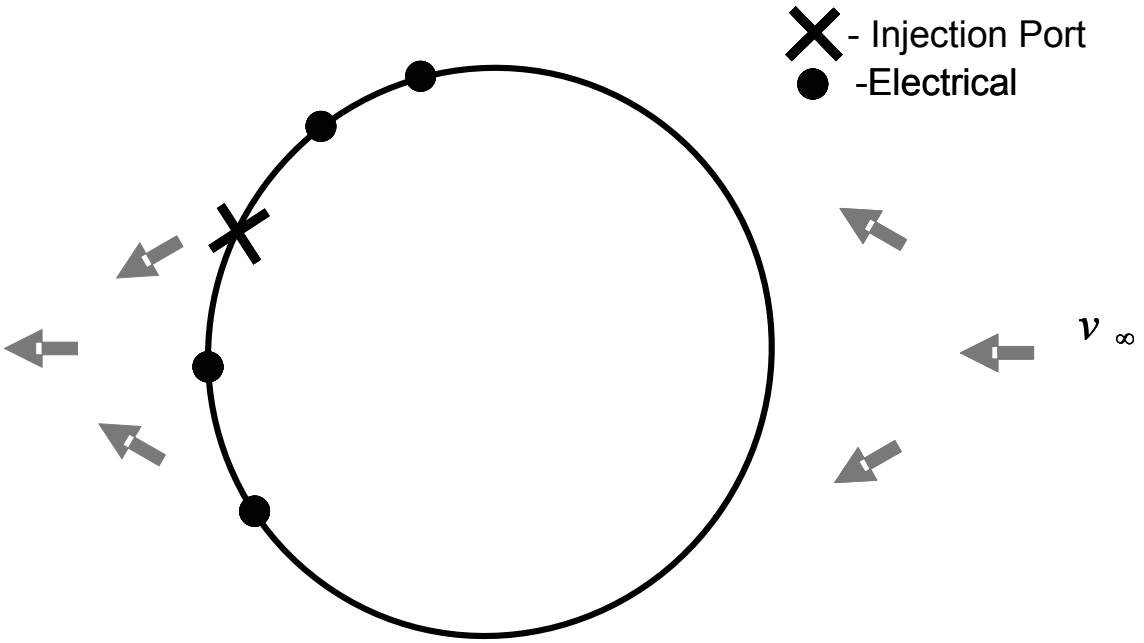

Figure 3.3 Flow around probe with injection port facing away from flow (previous design).

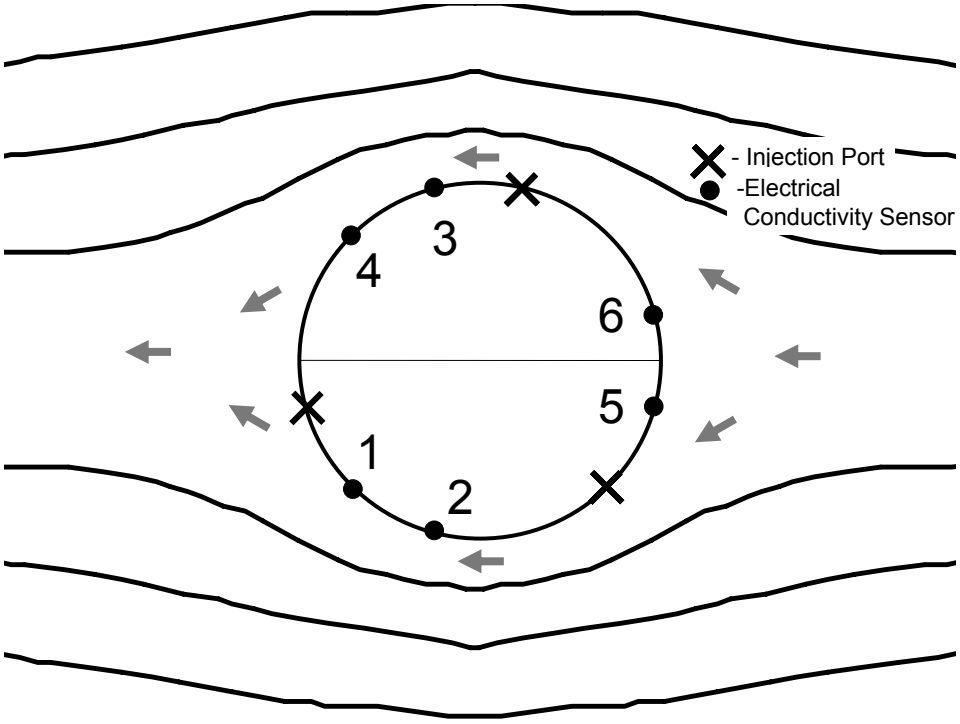

Figure 3.4 Redesigned location of injection ports and electrical conductivity sensors.

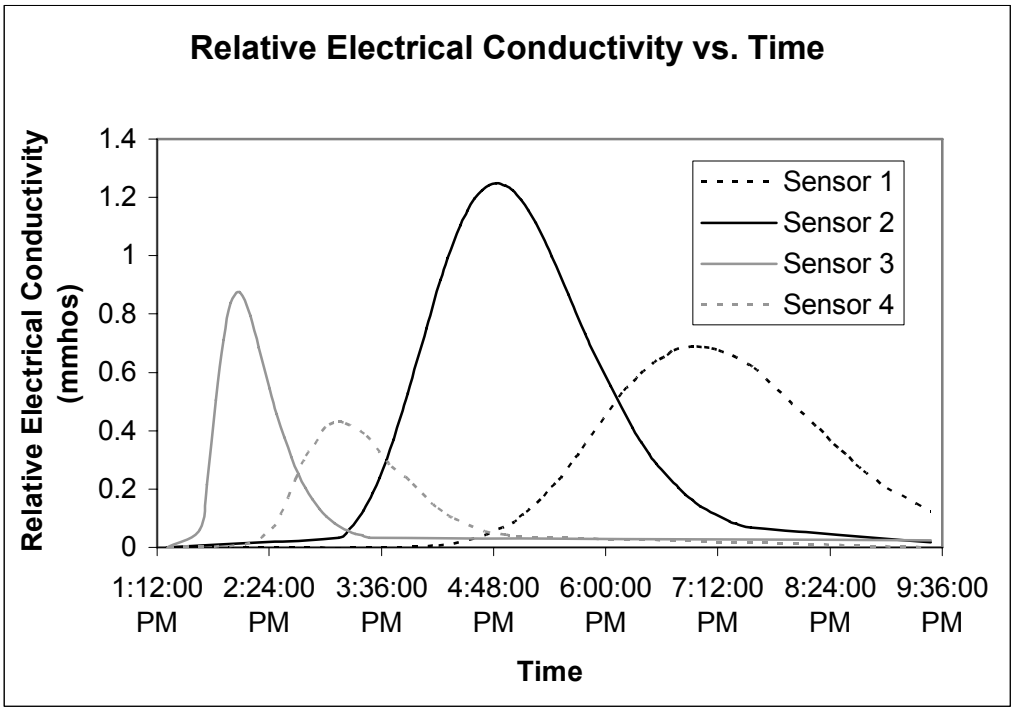

Figure 3.5 Typical breakthrough data for four sensors measuring two injections.

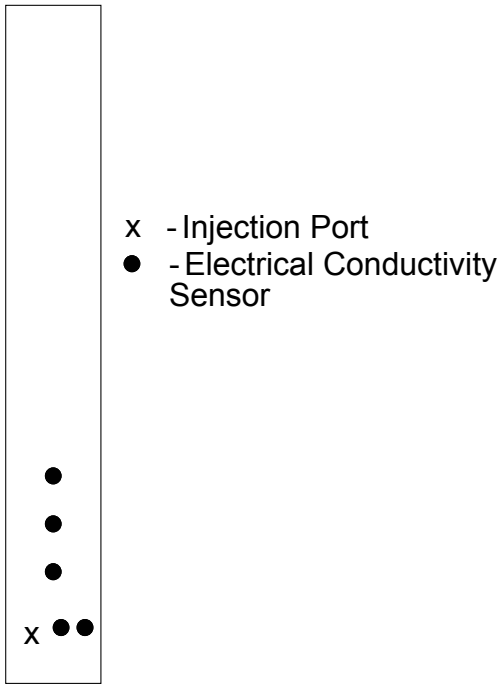

Figure 3.6 Electrical conductivity sensor location.

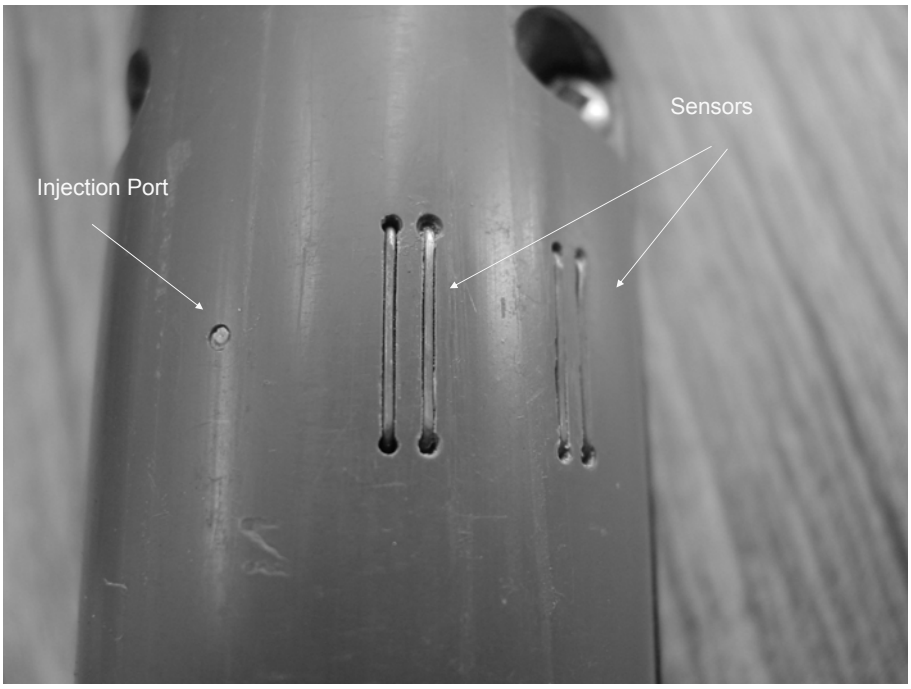

Figure 3.7 Close up of injection port and electrical conductivity sensors.

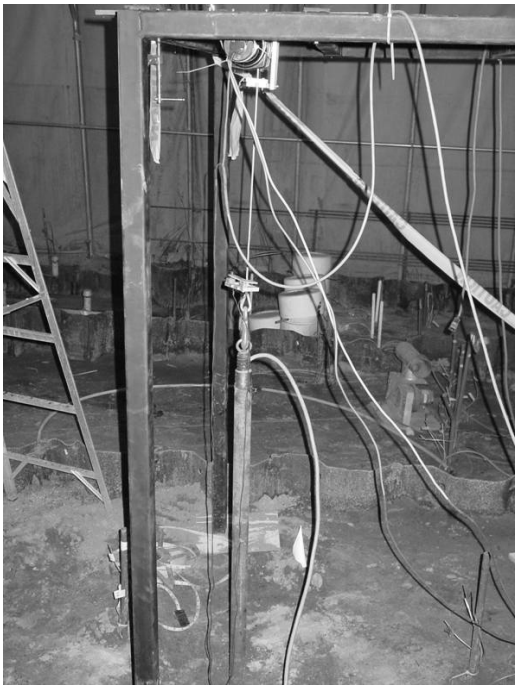

Figure 3.8 Winch and probe during field application.

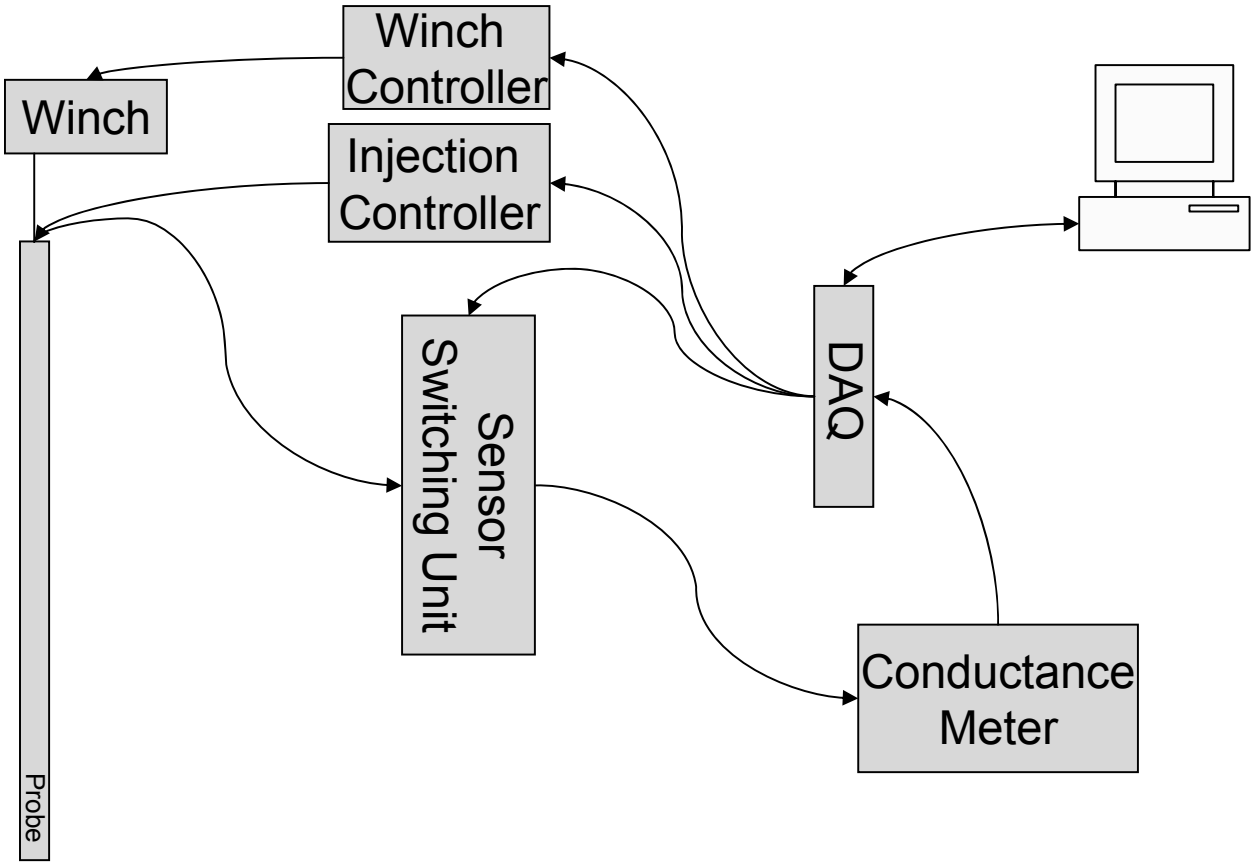

Figure 3.9 Flow chart of system operation.

4. Field Experiments

4.1 Introduction

The following objectives were pursued through a series of field experiments conducted between June 2006 and November 2006:

1) assess the performance of the new probe design;
2) assess the performance of the remote operation of the system; and
3) investigate groundwater flow in the near-water table region, focusing particularly on the capillary fringe.

4.2 Site Location and Description

This study was conducted in a controlled flow cell at Canadian Forces Base Borden (Borden), located approximately 70 km north-west of Toronto. Many researchers have studied both the geology and hydrogeology of this location (MacFarlane et al., 1983; Abdul, 1985; Mackay et al., 1986; and Sudicky, 1986).

The controlled flow cell used for these experiments was situated in the unconfined surficial aquifer composed of fine to medium grained sand (Mackay et al., 1986) which is approximately 3 to 3.5 m thick, and underlain by a regionally extensive clay aquitard (MacFarlane et al., 1983; and Brown et al., 1997). Despite commonly being regarded as a homogeneous aquifer, Sudicky (1986) found hydraulic conductivity values to range from 6 x 10^{-4} cm/s to 2 x 10^{-2} cm/s over vertical distances of less than 1 m.

Labaky (2004) conducted permeameter tests on soil cores and slug tests in boreholes to estimate the hydraulic conductivity in a controlled flow cell located adjacent to the cell used for these experiments. The average hydraulic conductivities of the permeameter tests conducted on two core samples were 6.06 x 10^{-3} cm/s and 6.13 x 10^{-3} cm/s. During this analysis, large differences (order of magnitude) for the hydraulic conductivity values were noticed over short vertical distances. It was hypothesized that this response was due to the

presence of 'small-scale interbedding'. Slug tests were performed in each borehole from which the cores were collected, giving hydraulic conductivity values of 5.68 x 10^{-3} cm/s and 5.82 x 10^{-3} cm/s.

Abdul (1985) measured the water content-pressure head relationship on samples taken from the unsaturated zone of the aquifer using the hanging water column method (Figure 4.1). From this data, it can be estimated that under drainage conditions the capillary fringe would extend approximately 30 to 40 cm above the water table while the interface zone may extend over 100 cm above the water table. Under conditions of a rising water table (wetting) the capillary fringe is smaller due to hysteresis and is predicted to extend less than 20 cm above the water table. From this water content profile Abdul (1985) calculated the water content-hydraulic conductivity relationship for Borden sand using the van Genutchten relationship (van Genuchten, 1980). See Figure 4.2.

The controlled flow cell is a section of aquifer closed on three sides by sheet-pile walls driven into the underlying clay aquitard. The dimensions of the cell are 25 m long by 2 m wide and approximately 3.5 m deep. See Figure 4.3 for a schematic of the cell and test locations within the cell.

Despite the experiments being performed in a controlled flow cell, it was not possible to control the position of the water table, which varies seasonally. Figure 4.4 shows the water table elevation at the groundwater velocity experiment location during the field experiment. In June, the water table was approximately 0.75 mbgs. It then dropped to a maximum of approximately 1.75 mbgs in early September before beginning to rise again in the fall in response to seasonal precipitation.

4.3 Field Experiments

Two types of experiments were conducted to investigate groundwater flow within the capillary fringe. Each type allowed for different parameters to be controlled.

The first set of experiments (*moving probe)* was conducted by installing the PVP below the water table and then measuring groundwater velocity at discrete vertical intervals while the probe was raised across the water table and into the capillary fringe. This type of experiment

allowed for some control over the location of the probe relative to the capillary fringe; however, it was not possible to account for the changes in groundwater flow caused by variations in geology.

The second type of experiment (*stationary probe)* was conducted over a 6 week period between September 2006 and November 2006. For this experiment the probe was positioned above the water table and remained stationary while seasonal recharge caused the water table and capillary fringe to rise past the probe. This method allowed for measurement of groundwater velocity both below the water table and in the capillary fringe while eliminating the uncertainty of changing geologic conditions associated with the *moving probe* experiments. However, it was still not possible to control the position of the water table relative to the probe with this experiment.

4.3.1 Average Cell Velocity and Correction for Storage

Flow through the controlled flow cell was regulated by pumping from a fully screened well (indicated as the extraction well in Figure 4.3) at the closed end of the cell. The average groundwater velocity within the cell (*average cell velocity*; *v*) was calculated using equation [13]:

$$v = \frac{Q}{A \times n} \qquad [13]$$

where

Q = rate at which water was extracted from the cell [L^3/T];

A = cross-sectional area available for flow through the cell (2 m wide by the thickness of the saturated zone, including an estimate of the capillary fringe thickness) [L^2]; and

n = porosity measured to be 0.33 (Mackay et al., 1986) [ ].

Equation [13] does not account for the effects of water released from storage or returned to storage when the water table elevation is changing rapidly. In the case of an unconfined aquifer, this release of water from storage is equivalent to the specific yield (S_y). For the Borden aquifer, the specific yield measured under field conditions is 0.25 (Nwankwor et al.,

1984). Thus for every meter of decrease in the elevation of the water table, an additional 0.25 m^3 (per square meter) of water is released due to drainage from the aquifer material (Figure 4.5). Conversely, under conditions of rapid water table rise, an equivalent amount of water will be taken into storage.

Equation [13] was modified to account for the effects of changing storage, [14]:

$$v_{corrected} = \frac{Q + \Delta S}{A \times n} \qquad [14]$$

where

ΔS = the rate of change in storage between the location of the probe in the flow through cell and the extraction well [L^3/T];

and ΔS is calculated by [15]:

$$\Delta S = \frac{\Delta h_{avg} \times A_{plan} \times S_y}{\Delta t} \qquad [15]$$

where

Δh_{avg} = the average change in the elevation of the water table over an interval of time (Δt) [L];

A_{plan} = the area over which the water table drops (2 m wide (cell width) by the distance between the probe and the end of the flow-through cell) [L^2];

These velocity values through the cell (*average cell velocity* and *corrected for storage*) are average values for the entire cross-section of the controlled flow cell and do not account for the effects of geology which may have different effects on velocity in different portions of the cell.

4.3.2 Installation Method and the Capillary Fringe

Labaky (2004) investigated the effects of different installation methods (those producing high hydraulic conductivity zones around the probe and those producing low hydraulic conductivity zones) on the measured groundwater velocity by modelling these scenarios using SALTFLOW 3.0 (Molson and Frind, 2002). Positive skins form when the probe is installed using a direct-

push method which causes compaction of soil around the probe and consequently a decrease in the hydraulic conductivity of this zone. Modelling results suggested that a positive skin "resulted in a proportional drop in the magnitude of velocity around the probe but direction was unaffected" (Labaky, 2004). Conversely, a negative skin is formed when the probe is installed in a manner that increases the hydraulic conductivity of the soil around the surface of the probe (e.g. water-jet installation). Labaky (2004) found that "negative skins resulted in an increase in the magnitude of the measured velocity by similar amounts." Based on these results, the installation method selected for these experiments was a water-jetting method described by Labaky (2004). An approximately 6 cm (2.5") O.D. casing was driven to the desired depth (50 cm to 100 cm below the water table) and the sand was then jetted from the interior of the casing using a garden hose. The PVP, attached to the drill rods, was then lowered down the casing which was subsequently retrieved, leaving the probe in direct contact with the aquifer material collapsed around it.

In order for the PVP to collect representative groundwater velocities, the surrounding geological material must collapse to be in direct contact with the PVP. During the installation, it is important that the distance between the probe and the inside of the casing is minimized, thus, limiting the amount of collapse that needs to occur for the probe to be in direct contact with the soil. However, if the space is too little, the possibility of a sand grain jamming between the probe and the casing exists.

Above the water table, capillary cohesion within the soil is suspected to prevent the aquifer material from collapsing against the probe (Fredlund and Rahardjo, 1993). Thus, three hypothetical situations for collapse around the probe above the water table can be envisioned (Figure 4.6):

i.) Case A: The water table is static and collapse occurs in the lower portion of the capillary fringe. This is suspected to only allow a small portion of the capillary fringe to be in direct contact with the probe.

ii.) Case B: The water table is falling, producing the largest capillary fringe (approximately 30 to 40 cm for Borden Sand (Figure 4.1)). The possibility for the entire capillary fringe to be in direct contact with the probe exists because soil

initially below the water table (in contact with the probe) will eventually be above the water table and still in contact with the probe.

iii.) Case C: The water table is rising. This produces the smallest capillary fringe (20 cm or less (Figure 4.1)). Since the soil around the probe in the capillary fringe must collapse as the water table raises, a limited portion of the capillary fringe is expected to be available to be measured by the probe.

4.3.3 Remote Operation and Data Collection

The depth of the water table at the location of interest was determined by interpolating water table elevations in adjacent monitoring wells. After determination of the water table elevation the probe was installed approximately 50 to 100 cm below the water table.

Once the probe was installed, it was possible to control all elements of data collection, tracer injection, and probe movement by using a program specifically written for this purpose (see Figure 4.7 for a screen shot of the remote system during data collection). Before groundwater velocity data was collected, electrical conductivity values were measured on several sensors until steady state values were reached. Often some drift occurred initially after installation which was attributed to the sensors being lightly abraded when the casing was withdrawn past the probe, thus, temporarily increasing sensor sensitivity.

When constant electrical conductivity values were reached, a 10 µl injection was performed from all three injection ports. This injection was controlled either on site or from a remote location over the internet by using remote desktop software. Immediately after the injection was performed, the collection of electrical conductivity data began. Electrical conductivity values were measured for a period of 15 – 30 seconds (per sensor) by a YSI-Model 32 Conductance Meter before being recorded to a spreadsheet. This time period was selected to allow the readings to stabilize before being recorded. After this preset period, of time the next sensor in the list of selected sensors was monitored. The sensors were continuously cycled through in this manner until the groundwater velocity reading was complete. As the data was collected, it was written to a spreadsheet and graphed in real time, thus allowing the user to visually monitor the data collection process. Once the user determined that a sufficient amount

of data were collected (approximately 75% of the last breakthrough curve), the data collection process was stopped and all of the data was automatically saved to a pre-assigned file.

Following data collection, the user could either repeat the velocity measurement at the same elevation or raise the probe to a new elevation and perform an additional velocity measurement. The winch, when operated by the program, would raise the probe a pre-set interval of either 2.5 or 5 cm. This was determined based on how the probe was connected to the winch. If the probe was connected directly to the winch cable it was raised in 5 cm intervals, however, if a pulley was connected to the probe, it was raised in 2.5 cm intervals. The use of the pulley not only increases the potential resolution of the vertical profile, but also has the added effect of doubling the maximum load of the winch. This can be important if the probe is installed in a tight formation or installed far below the ground surface where the effects of friction are significant.

Before raising the probe, the operator would view a webcam that was setup to monitor the site. This was to ensure that the probe was operated in a safe manner (the winch was free of people and obstructions) and to visually confirm that the probe moved to the new elevation. Once the probe was raised and the electrical conductivity values stabilized, the injection and data collection process was repeated.

4.4 Results

In the first set of measurements (*moving probe*), the probe was raised in an attempt to collect a vertical velocity profile across the water table and into the capillary fringe. In the second setup, (*stationary probe*) the probe remained stationary to allow for the fall recharge to raise the water table and capillary fringe past the probe. The ground surface within the flow through cell was not level, thus all depth measurements were taken relative to a datum (indicated in Figure 4.3). The level of this datum is referred to as ground surface and thus depth measurements are referred to as mbgs (meters below ground surface).

Moving Probe

A total of three moving probe experiments were conducted, with the first between June 6 and June 12, 2006.

June 6 – June 12

The probe was installed on June 6th 2006 to an initial depth of 1.59 mbgs. Figure 4.4 shows the location of the probe relative to the water table over the course of the test. Over the 6 day period of the test the probe was raised approximately 50 cm and groundwater velocity readings were collected. Also during this time period the water table declined by approximately 40 cm at the location of the probe due to seasonal drainage. During the water-jetting phase of the installation, pieces of organic matter were encountered. However, because of the installation method, it was not possible to determine the depth from which this material originated, making it difficult to correlate its presence to the recorded data.

Figure 4.8 shows the groundwater velocity measurements recorded during this test. Also shown is the *average cell velocity* calculated using equation [13]. Due to the rapid decline in the elevation of the water table over the duration of the test, the rate of extraction was adjusted in an attempt to maintain a constant average velocity through the cell. Equations [14] and [15] were used to account for the amount of water released from storage between the location of the probe and the extraction well due to the dropping of the water table. This *corrected for storage* value is also shown in Figure 4.8.

Groundwater velocity measurements recorded on sensor pair 1-2 range from a maximum of 55 cm/day to a minimum of 14 cm/day. The velocity measurements recorded by this sensor pair appear to agree best with the average cell velocity *corrected for storage*. These readings show a decreasing trend in velocity from approximately 1.6 to 1.2 mbgs. Above 1.2 mbgs this sensor pair was unable to measure groundwater velocity. The reason for this is unknown. At several depths multiple groundwater velocity readings were collected to investigate the reproducibility of the measurements. For this sensor pair, there was good agreement between multiple readings at the same depth with a minimum difference between repeated readings of 0.4 cm/day at 1.41 mbgs and a maximum difference of 14 cm/day at 1.36 mbgs. When compared to the *average cell velocity* and the *corrected for storage* velocity, the measurements

recorded on this sensor pair had a percent difference of approximately -26% and +5% respectively (Table 4.1).

Groundwater velocity measurements recorded using sensor pair 3-4 show much more scatter than those recorded by sensor pair 1-2. The maximum recorded velocity is 216 cm/day at 1.4 mbgs and the minimum is 15 cm/day at 1.15 mbgs. For unknown reasons this sensor pair was unable to measure groundwater velocity between 1.35 and 1.15 mbgs. Readings on this sensor pair were much less reproducible when multiple measurements were taken. At 1.41 mbgs a difference of approximately 140 cm/day was recorded while at the same elevation on sensor pair 1-2 a difference of 0.4 cm/day was recorded.

From each velocity reading, an accompanying direction (α) was calculated. Based on the orientation at which the probe was installed relative to the anticipated flow direction (oriented similar to Figure 3.4), the expected direction (α) for sensor pair 1-2 and 3-4 was -45° and 75° respectively. Recalling from Figure 2.2, α represents the angle between the injection port and the groundwater flow direction. Groundwater flow direction values in Figure 4.9 are near the expected values; however, both sensor pairs show a slight shift, indicating that flow may have been disturbed locally, or the probe may not have been oriented into the flow exactly as shown in Figure 2.2.

The decrease in the elevation of the water table during this experiment is expected to produce a situation similar to Case B (Figure 4.6). Thus, it can be anticipated that a large portion of the capillary fringe would be in contact with the probe. Nevertheless, only 1 data point was measured in the capillary fringe, approximately 10 cm above the water table (indicated as an asterisk (*) in Figure 4.8 and Figure 4.9). This value was measured on sensor pair 3-4 and is similar in direction and magnitude to velocity readings collected below the water table.

August 4 – August 17

The probe was installed on August 4th 2006 to an initial depth of 1.83 mbgs. Figure 4.4 shows the location of the probe relative to the water table over the course of the test. Over the 13 day period of the test the probe was raised approximately 28 cm and groundwater velocity readings were collected. During this time, the water table declined by approximately 20 cm at

the location of the probe due to seasonal drainage. Figure 4.10 shows the recorded groundwater velocity measurements recorded during this test; also shown is the *average cell velocity* calculated using equation [14]. During the test, the extraction rate decreased due to a pump malfunction; however, since the extraction rate is not monitored remotely, it is difficult to determine when the failure occurred. The dashed segment of the *average cell velocity* indicates the interval over which the pump failure occurred.

Since the water table was declining, an estimation of the amount of water released from storage between the location of the probe and the extraction well was calculated using equation [15] and an average velocity *corrected for storage* was calculated using equation [14], also shown in Figure 4.10.

Groundwater velocity measurements recorded on sensor pair 1-2 show very little variation with depth, with a maximum value of 9 cm/day and a minimum value of 7 cm/day. The velocity measurements recorded by this sensor pair are significantly less than the *average cell velocity* and are somewhat less than the average velocity when *corrected for storage*. During this test 3 multiple injections were performed to assess the reproducibility of the probe. The average difference between these multiple injections was 0.32 cm/day, indicating a high degree of reproducibility for this sensor pair.

In comparison, groundwater velocity measurements recorded on sensor pair 3-4 show more scatter than sensor pair 1-2, but much less than was seen during the previous test (*June 6 – June 12*). The maximum recorded velocity was 22 cm/day and the minimum was 7 cm/day. Readings on this sensor pair were reasonably reproducible when multiple injections were performed with a maximum difference of 5 cm/day and a minimum difference of 1.5 cm/day. For both sensor pairs, the amount of error between the measured and expected velocities decreased when the correction for storage was applied. These improved from an average percent difference of approximately -72% to approximately -47% for sensor pair 1-2 and from approximately -51% to +7% for sensor pair 3-4 (Table 4.1).

From each velocity reading, an accompanying direction value (α) was calculated. Based on the orientation at which the probe was installed relative to the anticipated flow direction (similar to Figure 3.4), the expected direction (α) for sensor pair 1-2 and 3-4 was -45° and 75°

respectively. Recalling from Figure 2.2, α represents the angle between the injection port and the groundwater flow direction. Groundwater flow direction values in Figure 4.11 are similar to the expected values with some scatter evident.

The decrease in the elevation of the water table over the duration of this experiment is expected to produce a situation similar to Case B (Figure 4.6). Thus, it can be anticipated that a large portion of the capillary fringe would be in contact with the probe. Despite anticipating a large portion of the capillary fringe to be measurable, velocity values were only measured up to 12 cm above the water table (indicated as an asterisk (*) in Figure 4.10 and Figure 4.11). These values are similar in direction and magnitude to velocity readings collected below the water table.

August 29 – September 13

The probe was installed on August 29th 2006 to an initial depth of 1.99 mbgs. Figure 4.4 shows the location of the probe relative to the water table. Over the 15 day period of the test, the probe was raised 40 cm and groundwater velocity readings were collected. The water table remained relatively stable over this period.

Figure 4.12 shows the recorded groundwater velocity measurements during this test. Also shown is the *average cell velocity* calculated using equation [13]. Since the water table changed little over the period of this test, no correction for the effect of water released from storage was calculated.

Groundwater velocity measurements recorded on sensor pair 1-2 range from a maximum of 16 cm/day to a minimum of 7 cm/day. The velocity measurements recorded on this sensor pair are approximately 10 to 15 cm/day less than the *average cell velocity*. Good reproducibility was achieved (5 cm/day or less) when multiple injections were performed at the same depth.

Groundwater velocity measurements recorded on sensor pair 3-4 range from a maximum of 34 cm/day to a minimum of 17 cm/day. This sensor pair shows more scatter than the data recorded by sensor pair 1-2. For three of the injections performed during this test, sensor 4 did not record the passing tracer pulse while sensor 3 did (indicated on Figure 4.12 as 'Sensor 3 Only'). These readings were interpreted using equation [7] by assuming the direction of flow

relative to the probe was equal to the installed orientation (α = 75º). One data point was recorded in the capillary fringe with this sensor.

From each velocity reading an accompanying direction (α) was calculated. Based on the orientation at which the probe was installed relative to the anticipated flow direction (similar to Figure 3.4), the expected direction (α) for sensor pair 1-2 and 3-4 was -45° and 75° respectively. Recalling from Figure 2.2, α represents the angle between the injection port and the groundwater flow direction. Groundwater flow direction values in Figure 4.13 are similar to the expected value for sensor pair 1-2, while the values for sensor pair 3-4 are approximately 40° greater than expected. This is interesting because sensor pair 3-4 measured groundwater velocity values closest to the calculated *average cell velocity* over the interval 1.85 mbgs to 1.75 mbgs.

The relatively stationary water table during this experiment is expected to have produced a situation similar to Case A (Figure 4.6). Thus, it would be expected that a relatively small amount of aquifer material would be in direct contact with the probe in the capillary fringe. One velocity value was measured 9 cm above the water table on sensor 3. Since the tracer pulse measured by sensor 3 was not measured on sensor 4 it is not possible to calculate a direction. However, if a flow direction is assumed (α = 75º based on installation orientation), it is possible to calculate the velocity. This velocity is similar to that measured by sensor pair 1-2 below the water table and slightly less than that measured by sensor pair 3-4 below the water table.

Stationary Probe

September 13 – November 1

The probe was installed on September 13th 2006 to an initial depth of 1.76 mbgs (immediately below the water table). On September 19th, the probe was raised to 1.58 mbgs at which point the electrical conductivity values at the level of the injection ports indicated that the probe was no longer in direct contact with the surrounding aquifer material. The probe was held stationary at this elevation for the remainder of the test while seasonal recharge raised the capillary fringe and water table past the probe. Over the 40 day period of the test, the water table rose 40 cm as shown in Figure 4.4.

Figure 4.14 shows the groundwater velocity measurements recorded over the duration of this test. Also shown is the *average cell velocity* calculated using equation [13]. Since the water table was rising at a variable rate during this test (i.e., faster during the second half of the test), the correction for storage was done over small intervals instead of applying an average for the entire duration of the test. The rate of water taken in by storage (ΔS) was calculated using equation [15]; the average cell velocity *corrected for storage* shown in Figure 4.14 was calculated using equation [14].

Groundwater velocity data collected on sensor pair 3-4 was approximately 10 to 15 cm/day greater than velocities measured on sensor pair 1-2 throughout the duration of the test. Velocity measurements made by both sensor pairs remained relatively constant for the first 30 days of the experiment. During the last 10 days of the experiment, the groundwater velocity readings began to increase. This trend is opposite to that predicted by the *average cell velocity* (equation [14]) which actually decreases towards the end of the experiment. However, when the effects of storage are accounted for, the velocity trend (*corrected for storage*) matches the shape of the trend seen in the recorded data. The percent difference between measured and expected velocity decreased significantly for sensor pair 3-4 when a correction for storage was applied (from +26% to +1%). However the percent difference increased for sensor pair 1-2. Despite this, the *corrected for storage* velocity matches the trend seen in the data measured on both sensor pair 1-2 and sensor pair 3-4.

Measured orientations (α) on both sensor pairs are clustered around the orientations that would be expected based on the orientation of the probe during installation (-45º for sensor pair 1-2 and 75º for sensor pair 3-4) as shown in Figure 4.15.

Three groundwater velocity readings were collected in the capillary fringe on sensor pair 3-4 between 3 and 5 cm above the water table, while no readings in the capillary fringe were collected on sensor pair 1-2. This suggests that collapse in the annular space around the probe under conditions of a rising water table (similar to Case C Figure 4.6) is limited. The first two velocity points recorded in the capillary fringe are slower than those measured below the water table. The third data point (closest to the water table) is similar in both magnitude and direction to that below the water table.

4.5 Discussion

The data collected as part of this field research addressed two main issues. The first was to assess the performance of the probe and the remote operation system and the second was to investigate groundwater flow conditions in the vicinity of the water table, specifically in the capillary fringe.

Probe Performance

Despite being difficult to quantify, operating the system remotely greatly increased productivity. Once installed, it was possible to collect data, perform injections and raise the probe remotely. As a result, over the duration of a test, site visits were only required to ensure that water was being extracted from the controlled flow-through cell at an appropriate rate (i.e. pump maintenance) and to collect water level data. If visits for these reasons had not been necessary, it would have been possible to only visit the site when it was time to install the probe in a new location, or refill the syringes.

Data collected on sensor pair 1-2 displayed a high degree of reproducibility, while data collected on sensor pair 3-4 was not as reproducible. Repeat measurements on sensor pair 1-2 were generally within 5 cm/day or less of each other. The measured orientations (α) show some scatter, however, they fall reasonably close to the expected orientation.

Over the duration of the test, sensor pair 3-4 consistently measured velocities greater than those measured on sensor pair 1-2. Since both sensor pairs were located in the same location relative to the flow, $\alpha + \gamma = 105^{\circ}$ for sensors 2 and 3, and $\alpha + \gamma = 135^{\circ}$ for sensors 1 and 4 (see Figure 3.4), it is unlikely that the orientation of the sensors to the groundwater flow was responsible for the discrepancy seen between the sensor pairs. However, the orientation of the injection ports to flow (α) differed, 45º for the injection port associated with sensor pair 1-2 and 75º for the injection port associated with sensor pair 3-4. This meant that the tracer pulse measured on sensor pair 1-2 traveled an additional 1.2 cm (30º) before being measured by the sensors. It is possible that the orientation to flow of the injection port, the additional flow distance, or a combination of these two phenomena was responsible for differences observed between the two sensor pairs.

Expected Velocity and Correction for Storage

When compared to the *average cell velocity* and the *corrected for storage* velocity, the measured data appears to fit best with the *corrected for storage* values. Notably, the *correction for storage* velocity matches the velocity trend evident in the stationary probe experiment where as the *average cell velocity* prediction did not. This result suggests that when experiments are conducted in controlled flows cells under conditions of a rapidly changing water table, the effects of storage need to be accounted for when estimating the expected rate of groundwater flow through the cell.

Table 4.1 shows the average percent difference between the measured velocities on each sensor pair and the *average cell velocity* and the *corrected for storage* velocity. When the entire velocity data set measured by the probe is compared to the *average cell velocity*, values recorded on sensor pair 1-2 were approximately 40% less than expected and values recorded on sensor pair 3-4 were approximately 15% greater than expected. When compared to the *corrected for storage* values, values recorded on sensor pair 1-2 were approximately 25% lower than expected and values recorded on sensor pair 3-4 were approximately 34% greater than expected. For sensor pair 1-2 an improved fit was achieved when a correction for storage was applied. For sensor pair 3-4 the quality of the fit decreased; however, this is due to the very high velocities measured during the *June 6 – June 12* experiment. When a correction for storage is applied to the rest of the experiments, an improved fit is achieved for sensor pair 3-4.

Predicted velocity values (*average cell velocity* and *corrected for storage*) are averages for the cross-section of the flow-through cell and assume homogeneous condition with uniform hydraulic conductivity and porosity. This assumption is not valid for the Borden aquifer because of the potentially wide range of hydraulic conductivity values Sudicky (1986). Thus the *average cell velocity* and the *corrected for storage* values should be used as a guide since point-to-point differences could be substantial.

For the moving probe tests, it can be reasonably anticipated that different hydraulic; conductivity zones will be encountered over the duration of the test (Sudicky, 1986) thus, different groundwater velocities can also be expected. However, the installation method used for installing the PVP does not allow for a determination of the geologic profile. Thus, the

scatter in some of the profiles can be expected to reflect changes in the hydraulic properties of the soil in contact with the probe.

Groundwater Flow in the Capillary Fringe

In all of the experiments, the PVP measured groundwater velocity above the water table in the lower portions of the capillary fringe (maximum of 12 cm above the water table) at magnitudes similar to those measured below the water table. However, the PVP was apparently unable to measure groundwater velocity in the upper portions of the capillary fringe. This is suspected to be a result of the cohesive forces present is soil located above the water table (Fredlund and Rahardjo, 1993) preventing the aquifer material from collapsing against the probe.

Three hypothetical collapse scenarios were proposed in Figure 4.6. Case B (falling water table) is expected to allow the largest portion of the capillary fringe to be measured by the probe. During the two tests that most resembled Case B, groundwater velocities in the capillary fringe were measured at maximum values of 10 cm and 12 cm above the water table. These are less than might be anticipated based on the amount of collapse that is expected to occur.

Case A (the case of a static water table) is expected to produce a range intermediate to Case B and Case C. One test similar to Case A was conducted and groundwater velocity was measured a maximum of 9 cm above the water table.

Case C is expected to produce the smallest thickness of measurable velocity in the capillary fringe because the soil must collapse as the water table rises. One test was similar to Case C and groundwater velocity was measured a maximum of 5 cm above the water table.

4.6 Conclusions

Based on the field research the following conclusions are drawn.

1) The new PVP design performed reliable injections and data collection. It exhibited a high degree of reproducibility; however, some difference between sensor pairs is evident. The difference between the measured velocity values and the calculated average groundwater velocity of the cell is likely a result of the heterogeneity of the Borden aquifer.

2) All aspects of the remote system operated successfully (tracer injections, data collection, and winch controlled probe movement). With all of these components operated remotely, it was possible to run the system for a period of at least a week without requiring a site visit. During these experiments the site was visited bi-weekly in order to ensure proper operation of the controlled flow cell.

3) The data collected from these experiments suggests that groundwater velocity in the lower portion of the capillary fringe is predominantly horizontal (when no sources of recharge are present) and is similar in magnitude and direction to that below the water table.

   All of the experiments demonstrated the ability of the PVP to measure groundwater velocity in the lower portion of the capillary fringe (up to 12 cm above the water table). However, the installation method (water-jetting) appears to limit the PVP's effectiveness in the capillary fringe. Installing the probe under conditions of a declining water table produces the largest measurable capillary fringe in contact with the probe.

4) These experiments, particularly the *stationary probe* experiment, illustrate the importance of correcting for the effects of storage in the controlled flow cells at Borden when the elevation of the water table is changing rapidly.

	Percent Difference			
	vs. Average Cell Velocity		vs. Corrected for Storage	
	Sensor 1-2	Sensor 3-4	Sensor 1-2	Sensor 3-4
June 6 - June 12	-25.9	87.7	4.9	165.6
Aug 4 - 17	-71.8	-50.9	-47.4	-6.5
Aug 29 - Sept 12	-57.3	-25.0		
Sep 13 - Nov 1	-18.3	26.4	-34.9	1.2
Whole Data Set	-39.3	15.3	-25.5	34.2

Table 4.1 Percent difference between measured velocity and expected velocity.

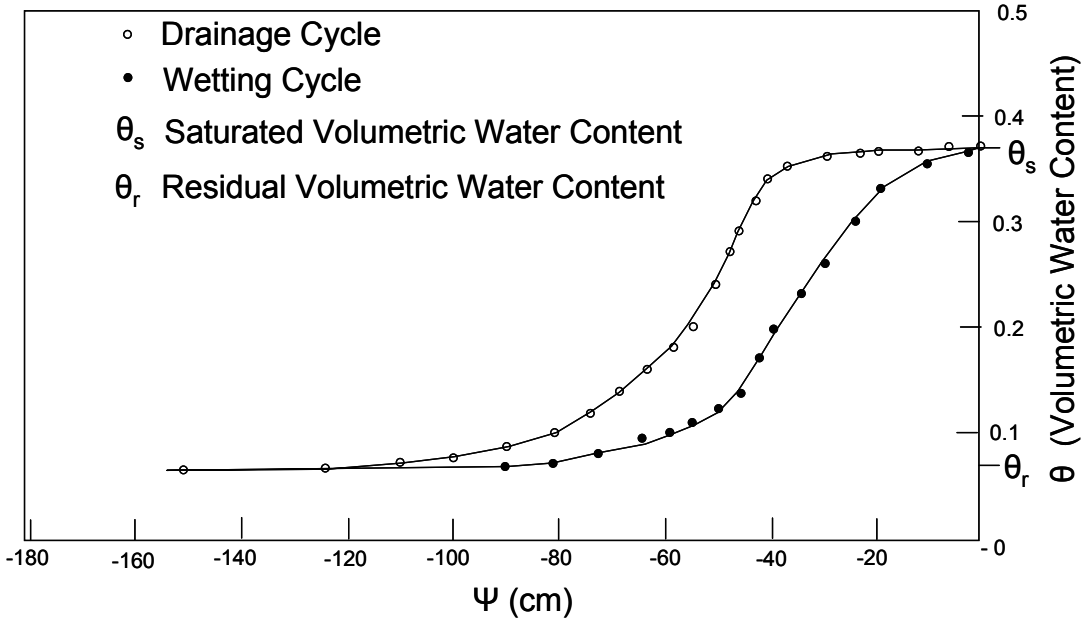

Figure 4.1 Pressure head – volumetric water content relation for Borden Sand (Abdul, 1985).

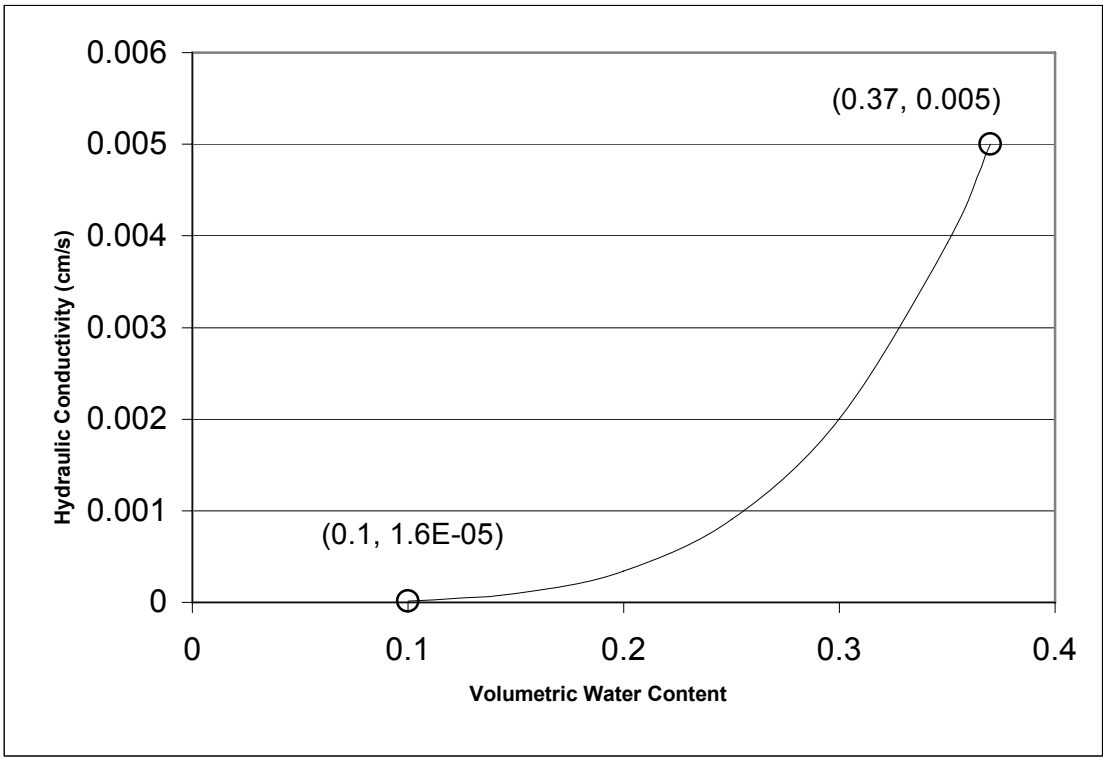

Figure 4.2 Volumetric water content – hydraulic conductivity relation for Borden Sand (Abdul, 1985).

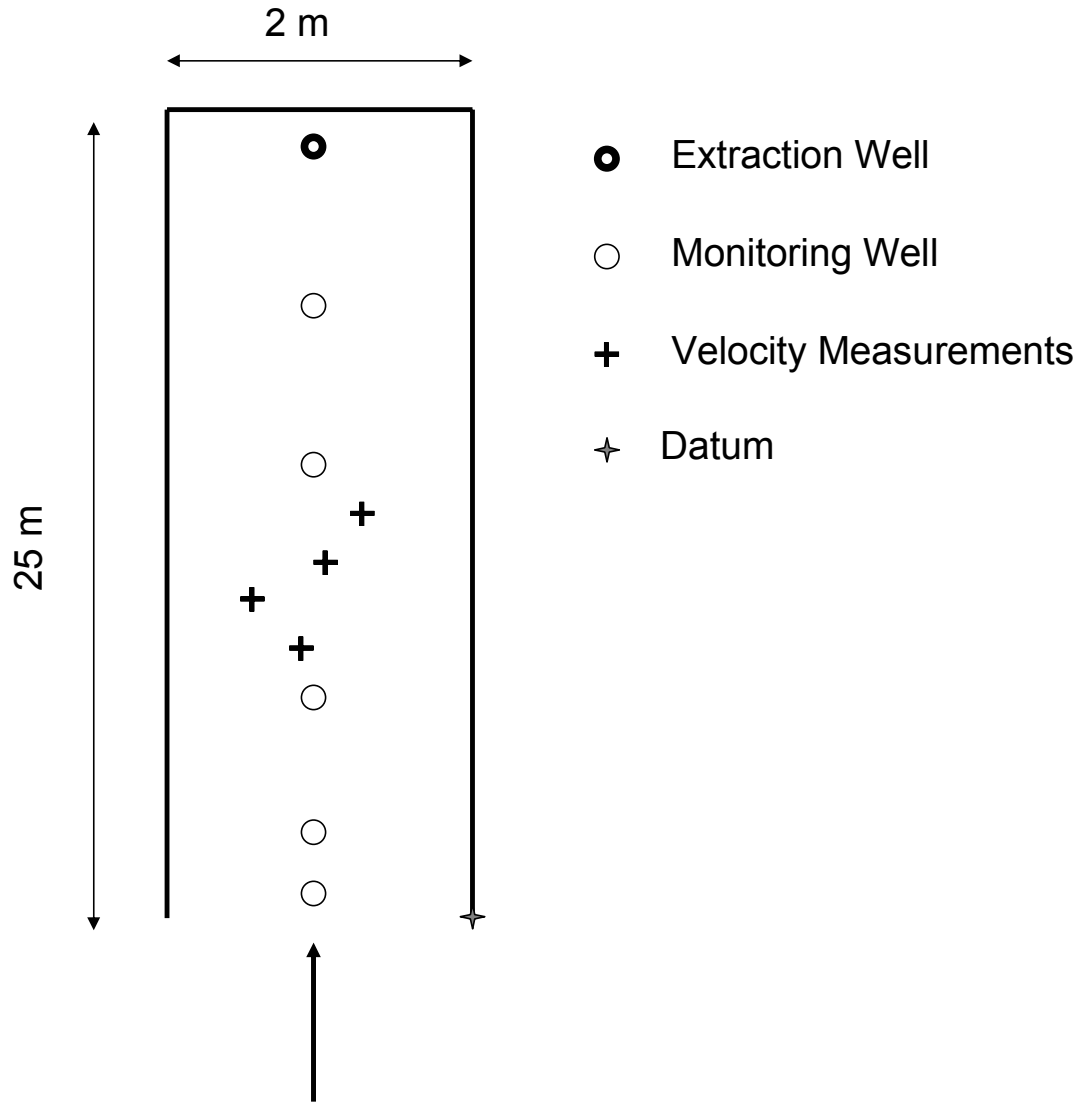

Figure 4.3 Controlled flow cell layout.

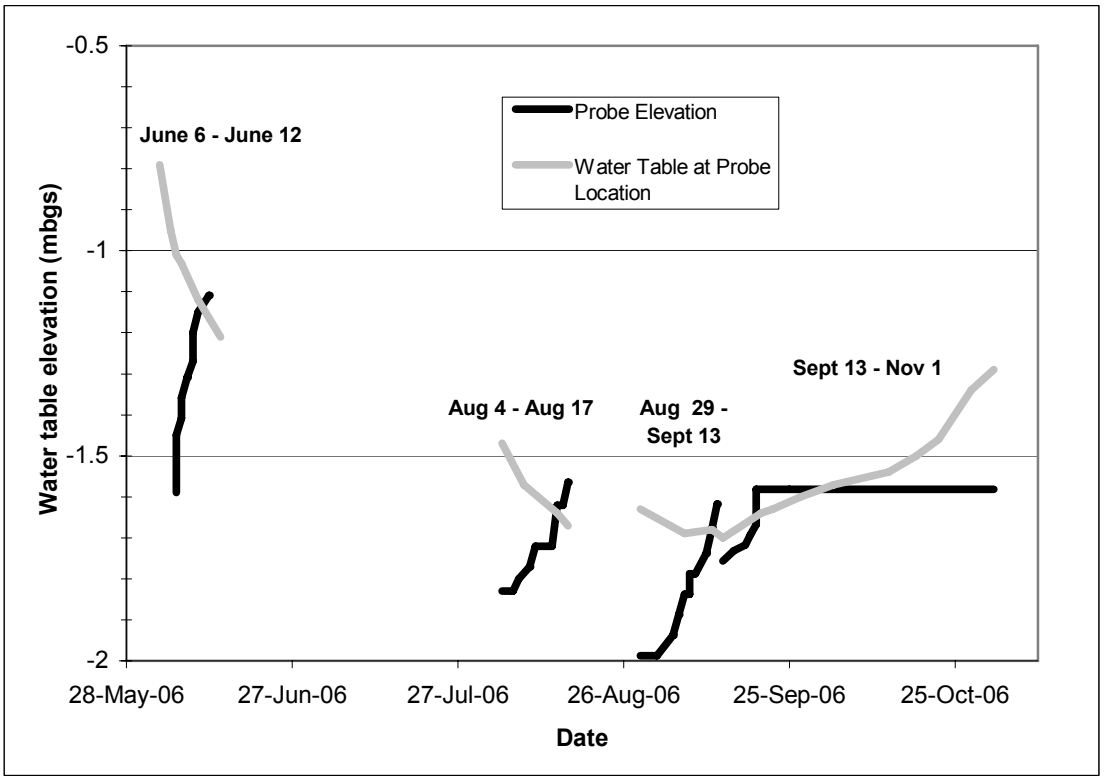

Figure 4.4 Controlled flow cell hydrograph and probe position.

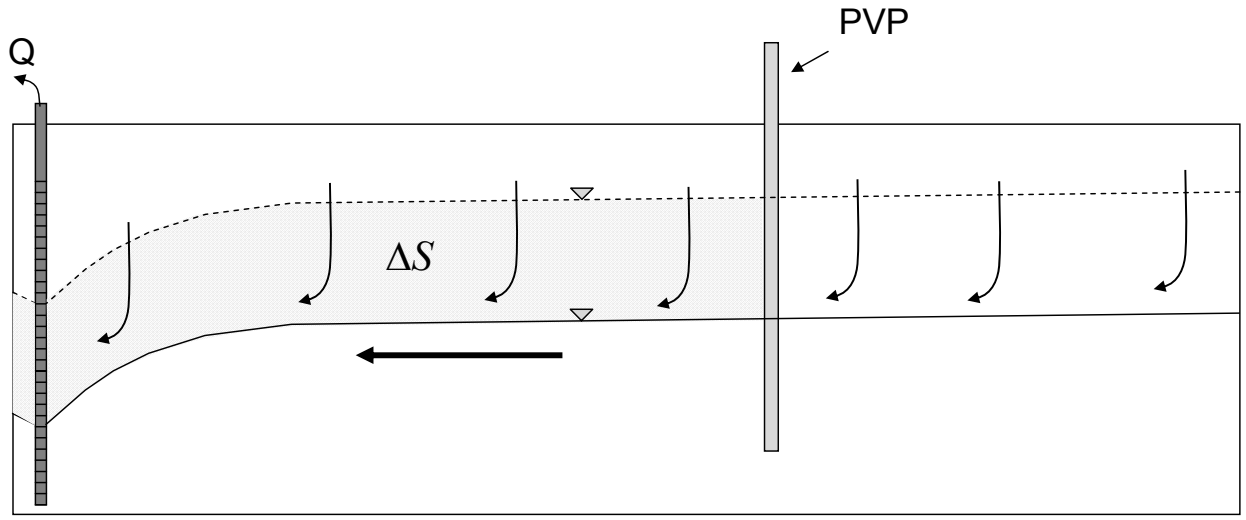

Figure 4.5 Contribution of storage to groundwater flow.

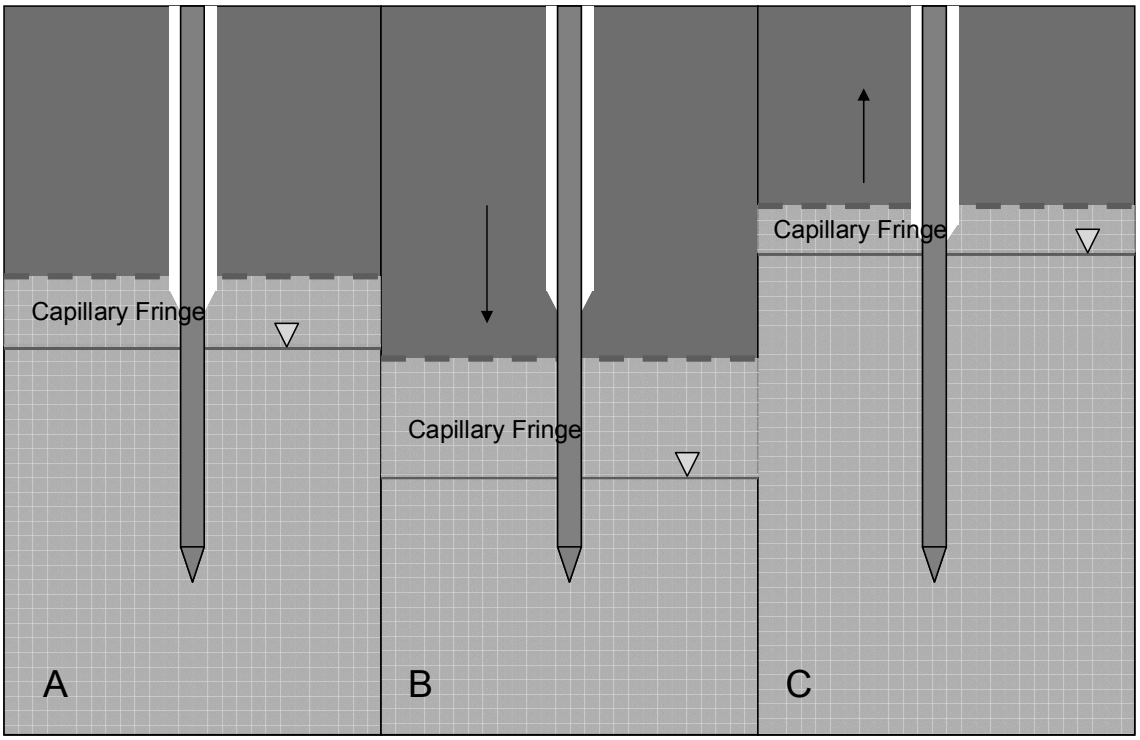

Figure 4.6 Hole collapse scenarios depending on water table movement.

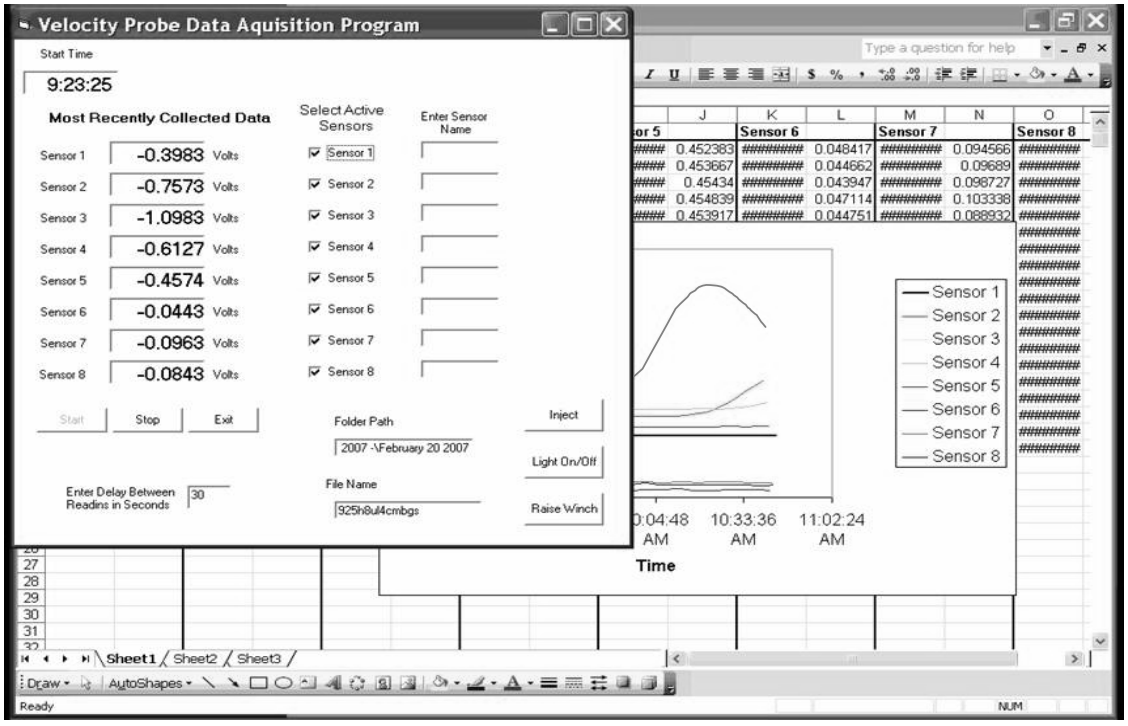

Figure 4.7 Screen shot of remote system interface with data being collected.

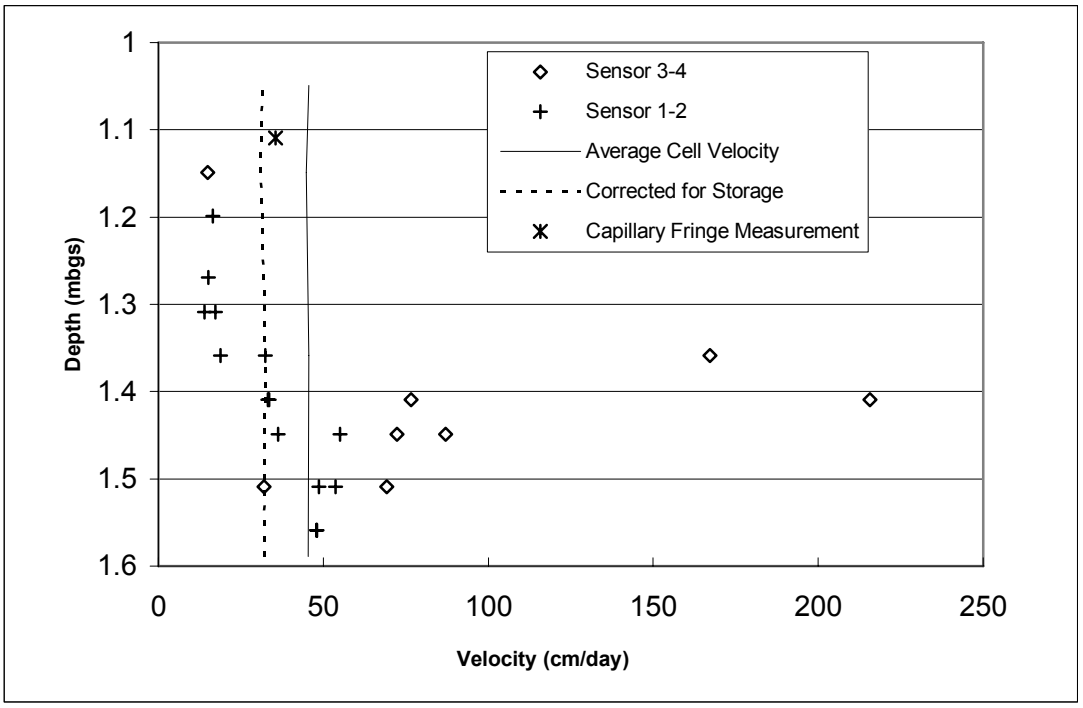

Figure 4.8 Vertical velocity profile, June 6 – June 12 2006.

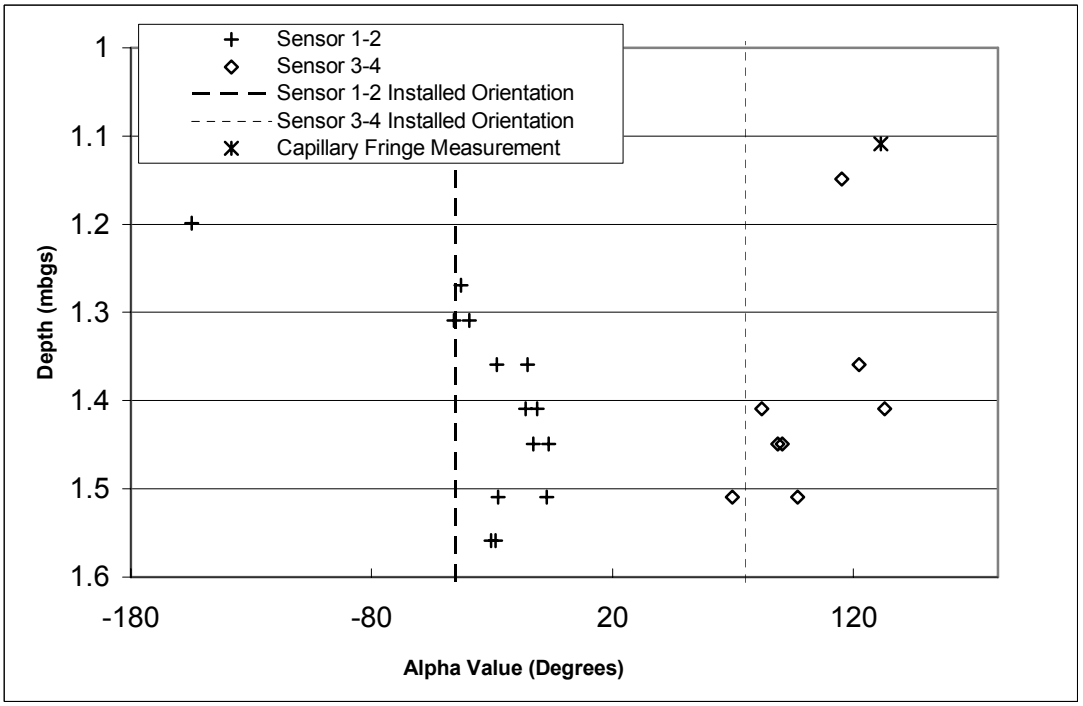

Figure 4.9 Flow direction vs. depth, June 6 – June 12 2006.

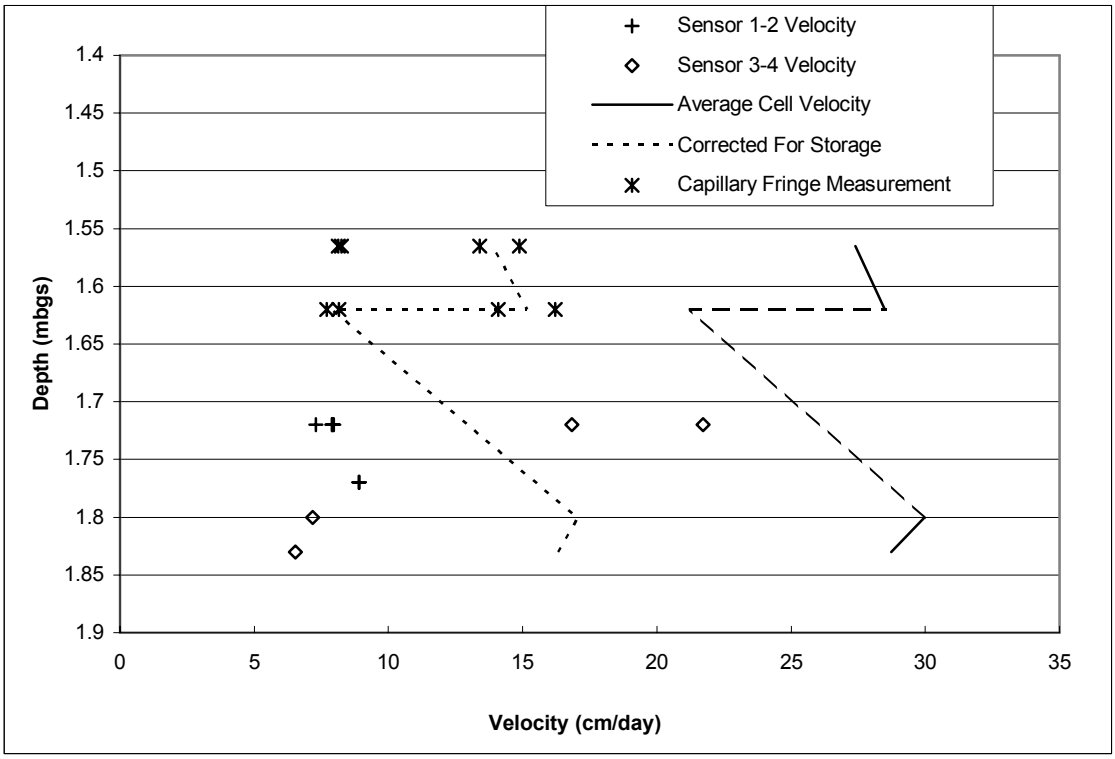

Figure 4.10 Vertical Velocity Profile, Aug 4 – Aug 17 2006.

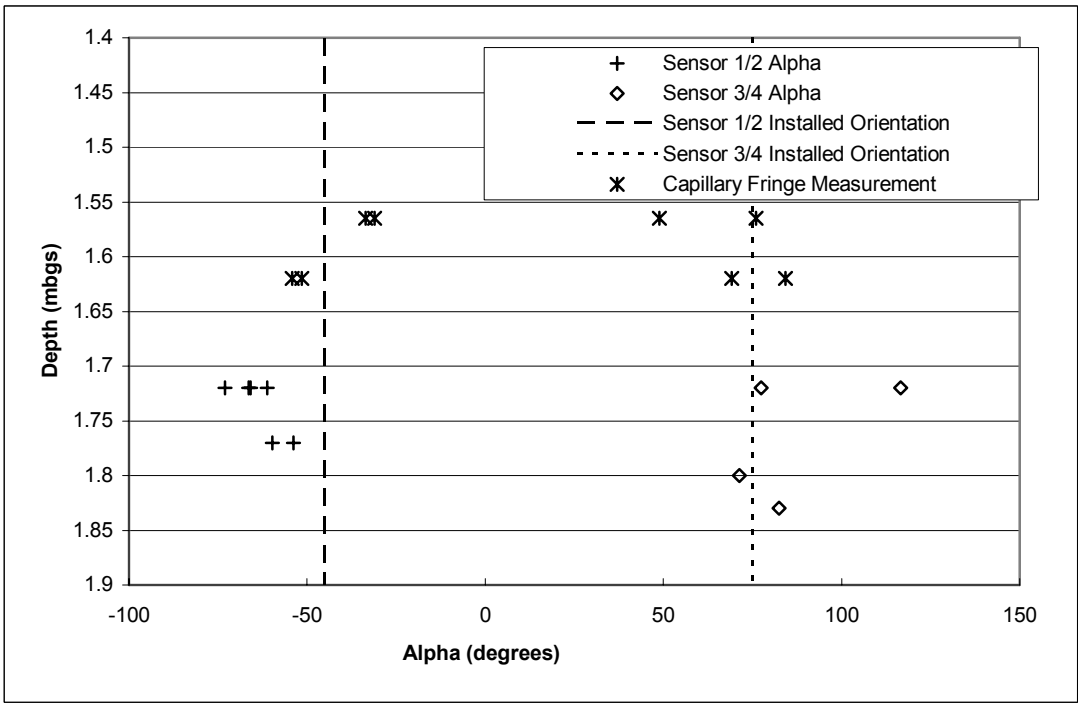

Figure 4.11 Flow direction vs. depth, Aug 4 – Aug 17 2006.

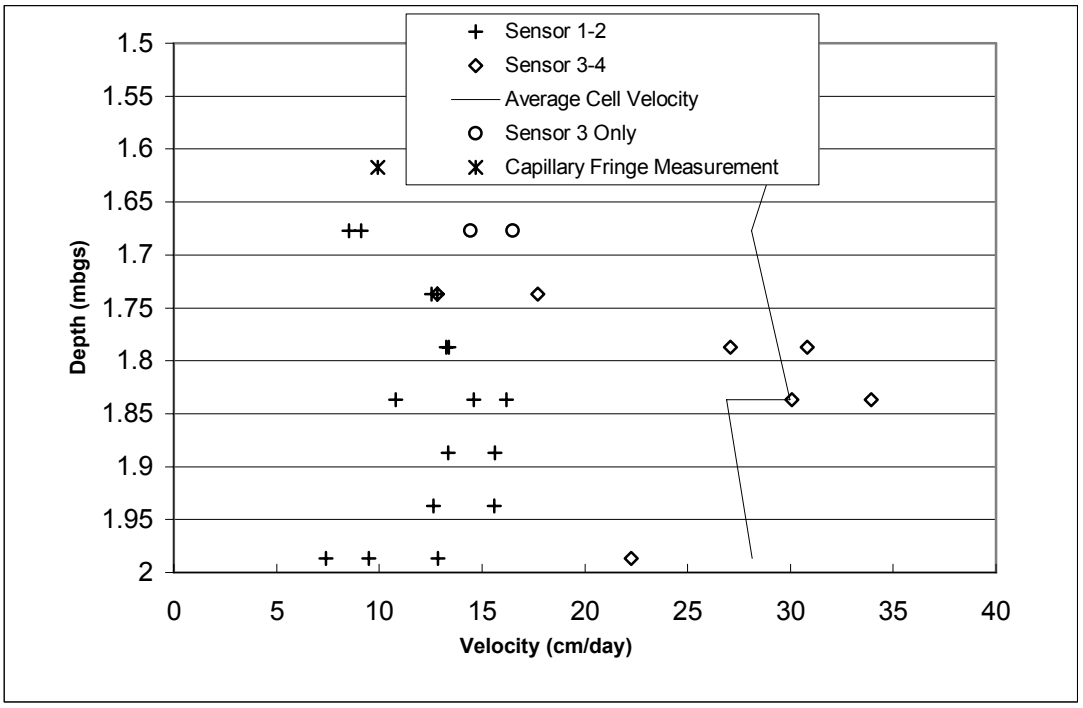

Figure 4.12 Vertical velocity profile, Aug 29 – Sept 12 2006.

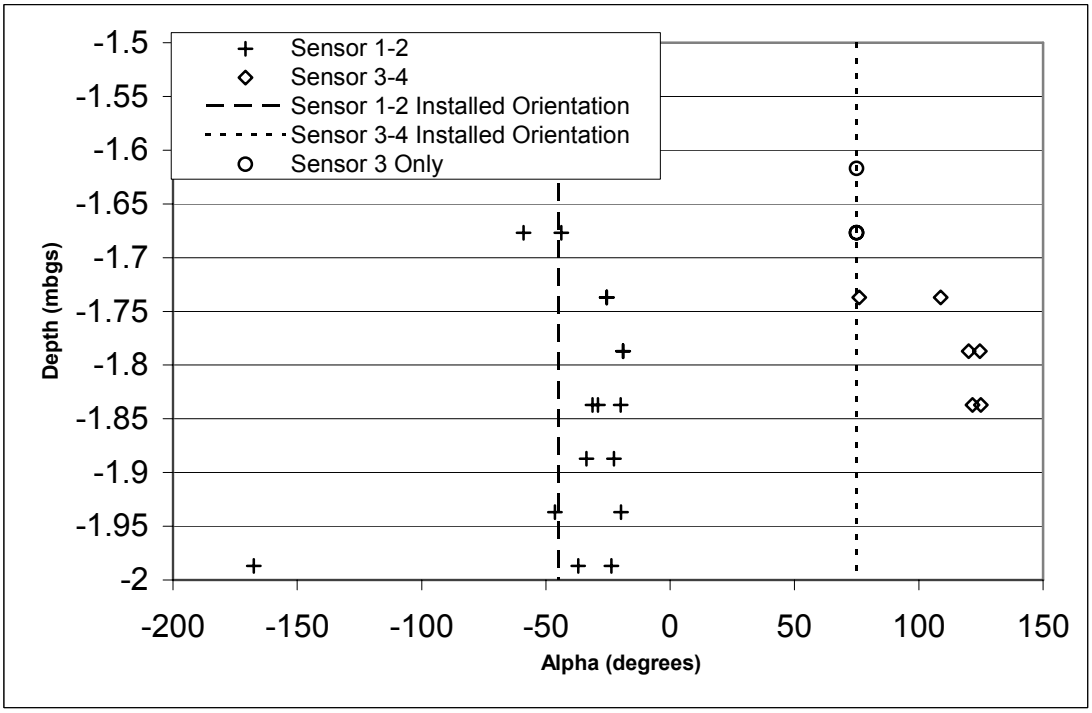

Figure 4.13 Flow direction vs. depth, Aug 29 – Sept 13 2006.

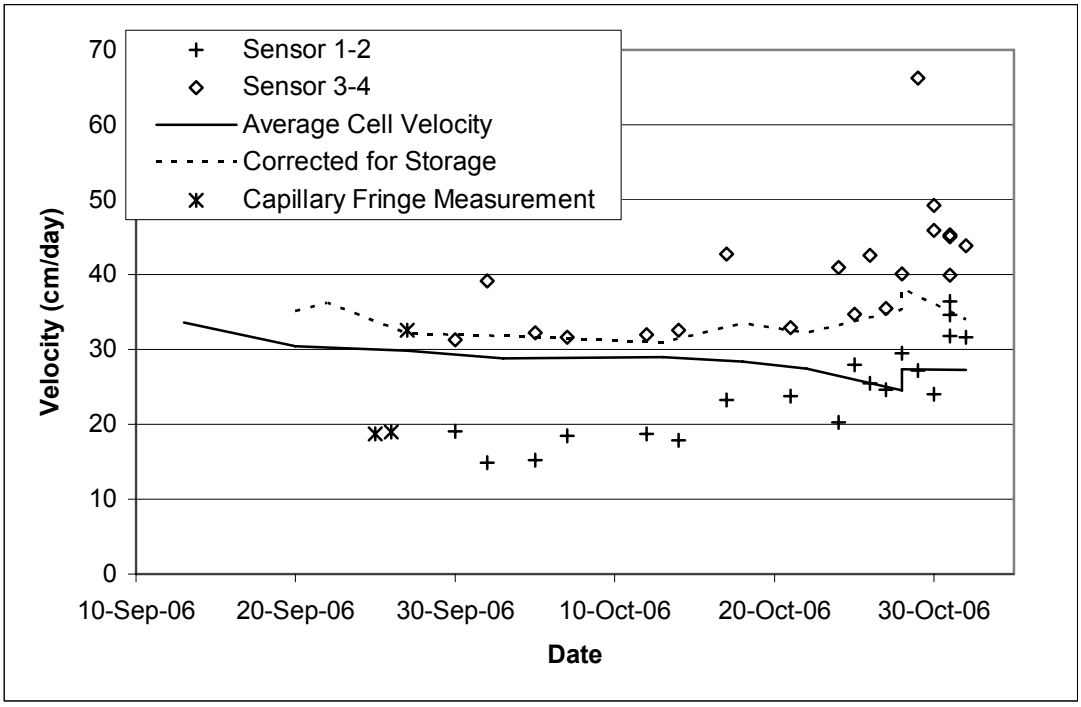

Figure 4.14 Groundwater velocity vs. time, Sept 13 – Nov 1 2006.

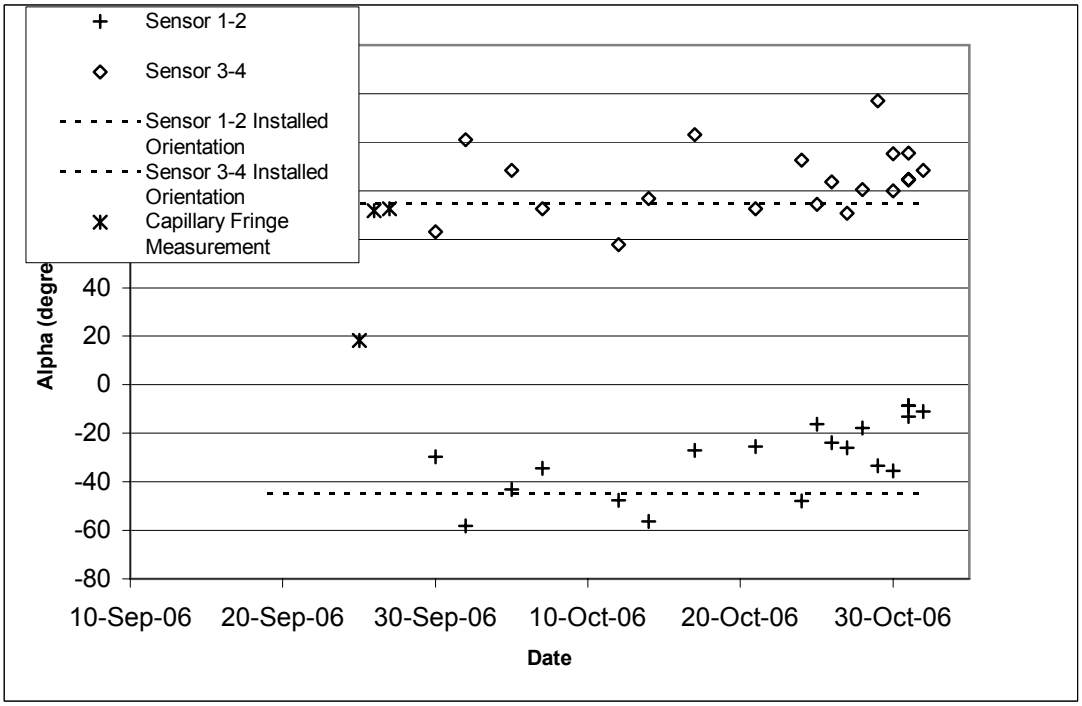

Figure 4.15 Flow direction vs. time, Sept 13 – Nov 1 2006.

5. Laboratory Experiments

5.1 Introduction

The ability of the probe to measure groundwater velocity in the upper portion of the capillary fringe during field investigations was suspected to be limited by the installation method. Results from the lower portion of the capillary fringe suggest that groundwater velocity is consistent in both magnitude and direction across the water table. To gain a better understanding of the results collected in the field, and particularly to examine the capability of the probe under more highly controlled conditions, laboratory experiments were designed to investigate the following:

1. the ability of the PVP to measure groundwater velocity over the vertical extent of the capillary fringe; and
2. the effects of drainage and wetting on groundwater velocity in the capillary fringe.

5.2 Methods

Experiments to investigate groundwater velocity in the capillary fringe were conducted in a 60 cm long flow tank constructed from 1.9 cm (0.75") thick plexiglass. The tank had an internal cross-section measuring 30 cm by 30 cm. At each end of the tank porous stainless steel plates mounted to 1.9 cm (0.75") thick plexiglass sheets were inserted. These inserts were constructed by hollowing the face of a piece of 30 cm by 30 cm plexiglass to create a reservoir. On top of this cavity a piece of 29 cm by 29 cm porous steel plate (Mott Corporation) was attached and the edges sealed. See Figure 5.1.

The hydraulic gradient across the tank was created by adjusting the hydraulic head in the reservoir behind each of the porous steel plates. The hydraulic head at the influent end of the tank was set using an overflow constant head device, and the hydraulic head at the effluent end was set using a drip point. By adjusting the position of each, it was possible to adjust the gradient, as well as raise and lower the water table. To ensure that flow through the tank was

parallel to the long axis, the tank was inclined to match the hydraulic gradient. See Figure 5.2 for a schematic of the tank and Figure 5.3 for a picture of the tank as setup in the lab.

The tank design was selected to avoid vertical flow in the capillary fringe near the inlet and outlet ends of the tank as witnessed by Wyckoff (1932) and Silliman (2002). Using the porous steel plates is advantageous because the capillary fringe is fully developed and flow is horizontal as soon as water passes through the plates and into the tank. In addition, it is possible to simulate regions above that water table greater than the depth of the tank.

To measure the volumetric water content, the tank was instrumented with 14 time-domain reflectometry (TDR) probes. Each probe was constructed from 2 pieces of 3.2 mm (1/8") stainless steel rod spaced approximately 3.2 cm apart in accordance with the 1:10 ratio recommended in (Knight, 1992). The probes were arranged in two groups of seven probes. Group 1 was located 19 cm from the influent end of the tank and Group 2 was located 19 cm from the effluent end. Within each group the probes were identified by the letters A – G. Probe A in each group was located 3 cm from the top of the tank, and Probe G was located 27 cm from the top of the tank. The remaining probes were spaced at 4 cm intervals in between (see Figure 5.2 and Figure 5.3). TDR traces were collected using a Tektronix 1502B Metallic TDR Cable Tester and interpreted using WinTDR (Or et al., 2003).

The tank was filled with air-dried sand collected from the surficial aquifer at CFB Borden. To avoid air entrapment and minimize the development of bedding during filling, the sand was mixed as it was added to water in the tank. The PVP was in place in the tank prior to the addition of the sand in order to eliminate disturbances that would have been caused if the probe had been installed after the tank was filled.

The PVP was located in the center of the tank with the injection ports and sensors for measuring groundwater velocity located 7 cm below the top of the sand, at the same elevation as TDR probes 1B and 2B. See Figure 5.2.

The initial experiment was conducted using a porous steel plate with pore sizes as great as 40 μm (bubble point measured to be approximately 28 cm). During laboratory flow tests these plates were able to hold 29.5 cm of tension before draining. This allowed for groundwater velocity measurements to be taken 22.5 cm above the water table.

To investigate regions greater than 22.5 cm above the water table, porous steel plates with 5 μm pores were used (bubble point measured to be greater than 70 cm). However, due to material availability it was necessary to reduce the internal width of the tank from 30 cm wide (as used for the 40 μm steel plates) to 24 cm wide.

Initially the water table was set near the top of the tank and the hydraulic gradient was adjusted until a suitable flow rate was achieved. The water table was then lowered in increments and a groundwater velocity reading was collected at each interval. The average velocity through the tank was calculated by [16]:

$$v = \frac{Q}{A \times n} \qquad [16]$$

where

v = average tank velocity [L/T];

Q = the measured flow rate at the effluent end of the tank [L^3/T];

A = the cross-sectional area of the tank [L^2]; and

n = porosity [ ].

Since the presence of the probe reduces the available area open to flow, a correction factor was applied to the measured velocities. This correction factor was based on an estimate of the expected increase in the average tank velocity caused by the decrease in area open to flow. However, since everything except the location of the water table is constant throughout the duration of the experiment, the trend in velocity measured by the probe can still be compared to changes in water content and pressure head.

After a velocity reading was recorded, the water table was adjusted to a new elevation and both the flow rate and water content values were allowed to stabilize before a new velocity measurement was taken. In both experiments, the water table was initially near the top of the tank and then lowered in steps.

5.3 Results

Two experiments were conducted, each using porous steel plates with different maximum pore sizes (40 μm and 5 μm).

5.3.1 40 μm Drainage Experiment

For this experiment, the probe was located 7 cm below the top of the tank at the same elevation as TDR probes 1B and 2B. The water table was initially set 5.5 cm above the injection ports and was then lowered in 2 cm intervals to 29.5 cm below the top of the tank (22.5 cm below the water table). Based on the pressured head-water content curve measured by Abdul (1985) this is expected to be within the lower half of the capillary fringe.

Figure 5.4 shows the groundwater velocity measurements recorded for this test and the water content measured on TDR probes 1B and 2B. Over this pressure head interval the water content values measured at the same level as the probe remained constant, as well as the groundwater velocity readings. The data show good agreement between the velocity values measured on sensor pair 1-2 and sensor pair 3-4.

The *average tank velocity* shows some variability due to degassing in the flow lines which resulted in a reduction in flow. However, the probe shows a high degree of sensitivity to these changes in tank velocity. Furthermore the measured velocities were reasonably close to the average velocity (generally within 2 cm/day).

Figure 5.5 shows that the measured orientations also closely match the expected values of -45° for sensor pair 1-2 and 75° for sensor pair 3-4.

Groundwater velocities recorded during this test indicated that velocities in the capillary fringe (up to 22.5 cm above the water table) are of the same magnitude and direction as those measured below the water table.

5.3.2 5 μm Drainage/Wetting Experiments

This experiment was conducted in two stages, *drainage* and *wetting*. During the *drainage* experiment, the probe was located 7 cm below the top of the tank at the same elevation as TDR

probes 1B and 2B. The water table was initially set to simulate the probe being located 2.5 cm below the water table. The water table was then lowered in 5 -10 cm intervals to an elevation of 86 cm below the top of the tank (equivalent to 79 cm above the water table at the location of the probe). After this elevation was reached the *wetting* experiment began. The *wetting* experiment measured groundwater velocity and water content values as the water table was raised.

5 μm - Drainage

Figure 5.6 shows the groundwater velocity measurements recorded for this test and the water content measured on TDR probes 1B and 2B. Water content values remained constant until a pressure head of approximately 60 cm was reached at the locations of the probe. As the pressure head decreased the water content values began to decrease due to drainage of the soil. Groundwater velocity readings showed more noise during this test despite the *average tank velocity* remaining relatively constant. Despite this scatter the velocity values are relatively constant up to 44 cm above the water table. At greater elevations above the water table, velocity values rapidly decreased until it was no longer possible to record flow at 68 cm above the water table.

Figure 5.7 shows the measured orientations for this experiment. The direction data shows more scatter than was seen in the *40 μm* experiment, however, the direction data remains clustered around the expected orientation. The decreased cross-sectional area of the tank used in this experiment may be responsible for the increase in scatter seen in both the velocity and orientation measurements.

Groundwater velocity up to 44 cm above the water table was consistent with velocity values recorded below the water table. At elevations greater than 44 cm above the water table the measured velocities decreased rapidly until flow was not measurable above 57 cm above the water table. The decrease in groundwater velocity precedes the decrease in water content by approximately 15 to 20 cm. This is suspected to be due to heterogeneity of the pore size distribution within the tank.

5 μm – Wetting

This experiment is a continuation of the drainage experiment with the only difference being the direction of water table movement. Figure 5.8 shows the groundwater velocity measurements recorded for this test as well as the water content measured on TDR probes 1B and 2B. Water content values increased slowly as the water table was raised to simulate the region between 80 and 50 cm above the water table. Between 50 and 35 cm above the water table, the rate at which the water content was changing increased. As the water table was raised further, the water content values remained constant at approximately 0.345, increasing slightly below the water table. This is in comparison to an initially saturated water content value of approximately 0.405 measured on the same TDR probes during the drainage experiment. At elevations greater than 21 cm above the water table groundwater velocity was not measured by the PVP. At elevations less than 21 cm above the water, groundwater velocity values slowly increased to a maximum of approximately 8 cm/day at 6 cm above the water table. This measured velocity value is in agreement with the average tank velocity; however it is approximately 3 - 5 cm/day (65 – 75% of original flow) lower than the velocities measured by the probe under initially saturated conditions during the drainage experiment.

Groundwater velocity data measured at a pressured head of -21 cm was only measured on sensor 3 for sensor pair 3-4. Thus, the data was interpreted by assuming an orientation to groundwater flow based on the orientation of the probe installation (75º for sensor 3).

Figure 5.9 shows the measured orientations for this experiment. This data is rather limited due to the small zone above the water table in which groundwater velocity was collected. The direction data shows more scatter than was seen in the *40 μm* experiment; however, the direction data remains clustered near the expected orientations. The decreased cross-sectional area of the tank used in this experiment may be responsible for the increase in scatter seen in both the velocity and orientation measurements.

The water content profile appears to be offset by approximately 15 to 20 cm in comparison to the measured velocities. This is similar to the trend witnessed in the drainage experiment. This is suspected to be a result of the heterogeneous distribution of pore sizes within the tank.

5.4 Discussion

Both drainage experiments (*40 μm* and *5 μm*) demonstrated the ability of the probe to measure groundwater velocity in the capillary fringe at elevations greater than were measured in the field. This supports the assumption that the absence of collapsed material around the probe was a major limiting factor to measuring flow in the capillary fringe under field conditions.

Under drainage conditions, groundwater velocity in the capillary fringe (up to 44 cm above the water table for this soil) is similar in both magnitude and direction to flow below the water table. Above this elevation groundwater velocity values decreased. During the *wetting* experiment, the region in which significant flow occurred was limited to within 5 to 10 cm above the water table. This is consistent with the wetting curve of the water content-pressure head relation for Borden Sand (Figure 4.1).

The hydraulic conductivity of the soil surrounding the probe during the *5 μm drainage* and *wetting* experiment was approximated in two ways (Figure 5.10). The first method was based on the pressure head – hydraulic conductivity relation calculated by Abdul (1985) (Figure 4.2). Assuming the repacked Borden sand used in the lab approximates the Borden sand used by Abdul (1985), a hydraulic conductivity was estimated using the water content values measured at sensors 1B and 2B.

The second method was to back calculate the hydraulic conductivity using the velocities measured during the experiment using equation [17]:

$$K = \frac{v \times n}{i} \qquad [17]$$

where

K = hydraulic conductivity [L/T];

v = velocity measured by the PVP [L/T];

n = tank porosity []; and

i = tank gradient [].

The calculated hydraulic conductivity values are slightly less than those predicted by using the pressure head – hydraulic conductivity calculated by Abdul (1985). Some difference between these curves is expected since the soil used is not the same as that used by Abdul (1985). Also, the artificial packing of the tank would be expected to introduce some error. The difference between the pressured head at which these curves begin to decrease (57 cm for (Abdul, 1985) and 44 cm for Sensors 1-2 and 3-4) is likely due to heterogeneities in pore size distribution within the tank. These curves demonstrate the sensitivity of hydraulic conductivity to changes in water content.

Scanning Curves

The set up of the tank allowed for the relationship between water content and pressure head at various degrees of drainage to be investigated. Thus, water content curves measured on different TDR probes represent simple scanning curves (Figure 5.11). The water content readings recorded on probes at similar elevations were averaged. The bold line (B Probe Average) represents the water content profile that was measured during the *5 μm Wetting* and *Drainage* experiments at the same elevation that velocities were recorded. Probes located nearest the top of the tank (*A Probe Average*) show the most air entrapment, and probes nearest the bottom of the tank (*G Probe Average*) show the least. This is as expected since more drainage and air entry is expected to occur near the top of the tank as it would have experienced more negative pressures relative to the bottom of the tank.

The continuity of horizontal flow observed in the capillary fringe during the *drainage* experiments may be of importance for the transport of contaminants in shallow unconfined aquifers. For example, in thin aquifers (less than 4 m thick), flow and transport in the capillary fringe may represent up to 10% of the flow (assuming a 40 cm capillary fringe). In case of very thin aquifers (2 m thick) this proportion increases to approximately 20%. The latter is similar to the surficial Borden aquifer during spring and summer months when the water table is low due to seasonal drainage.

5.5 Conclusions

The laboratory experiments demonstrate the ability of the probe to measure groundwater flow in the capillary fringe when in direct contact with the aquifer material. Under conditions of drainage, groundwater velocities of a magnitude similar to those below the water table were measured up to approximately 45 cm above the water table. Groundwater velocity values less than this were measured between 45 and 57 cm above the water table. This suggests that the inability of the probe to measure groundwater flow in the capillary fringe under field conditions is likely a result of the installation method.

Under wetting conditions the region in which groundwater flow occurs above the water table is limited in comparison to that measured under conditions of drainage. This agrees with the water content – hydraulic conductivity relationship calculate by Abdul (1985) for Borden sand. During the wetting experiment, a small amount of air entrapment was observed at the elevation of the probe as reflected by water content measurements. This difference in water content (presence of trapped air) is likely responsible for the difference between the measured velocities at similar pressure heads under conditions of drainage and wetting.

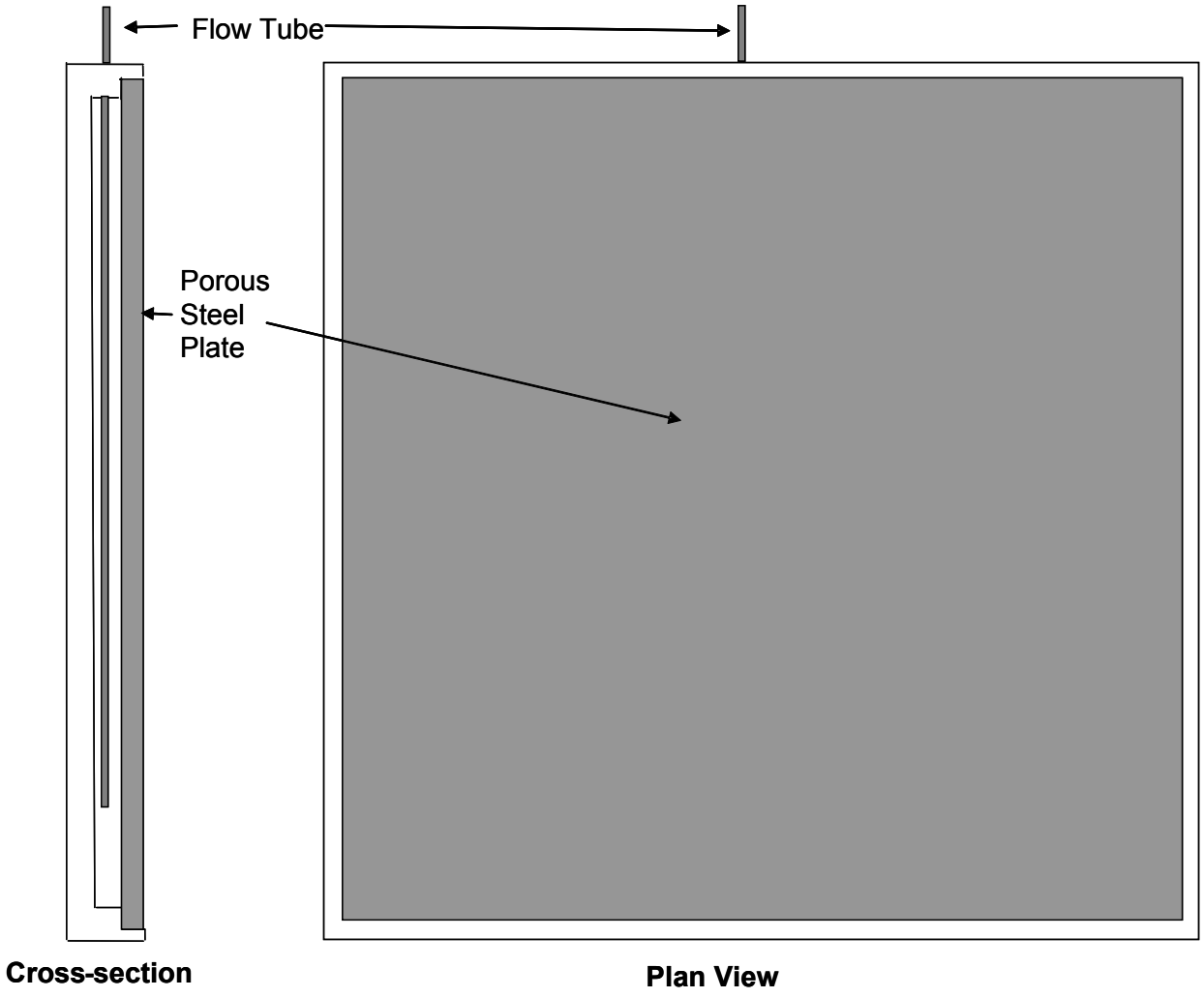

Figure 5.1 Porous steel insert – Cross-section and plan view.

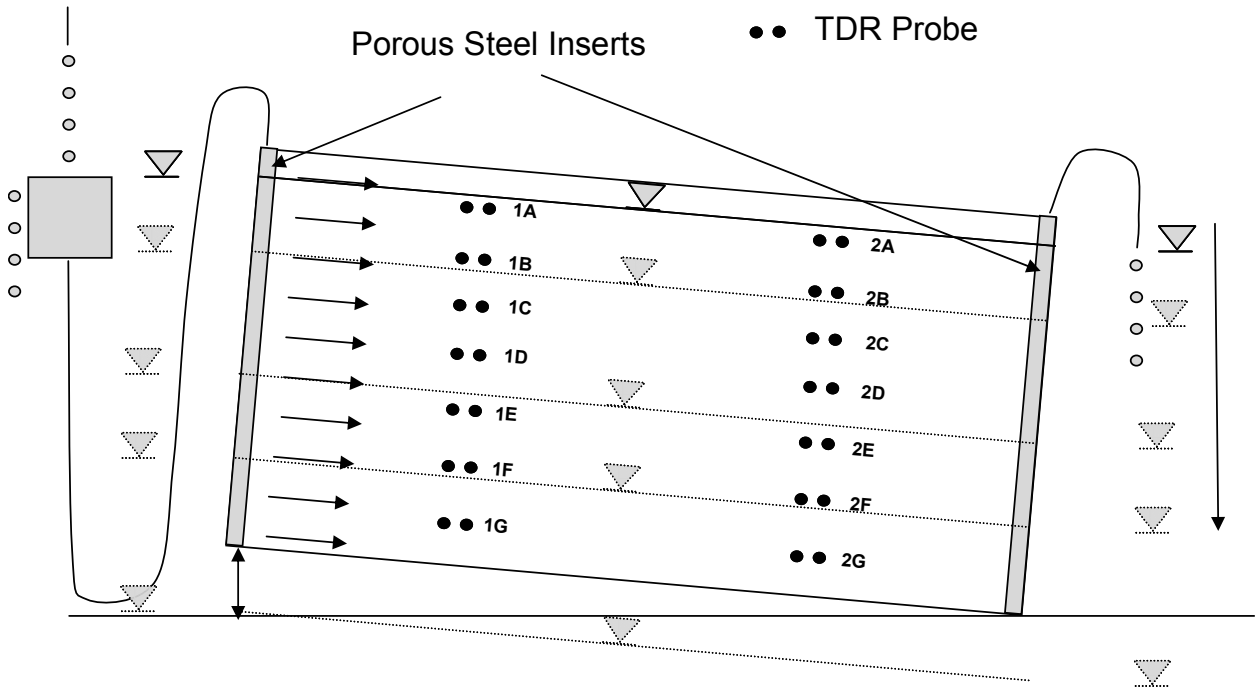

Figure 5.2 Flow through tank layout.

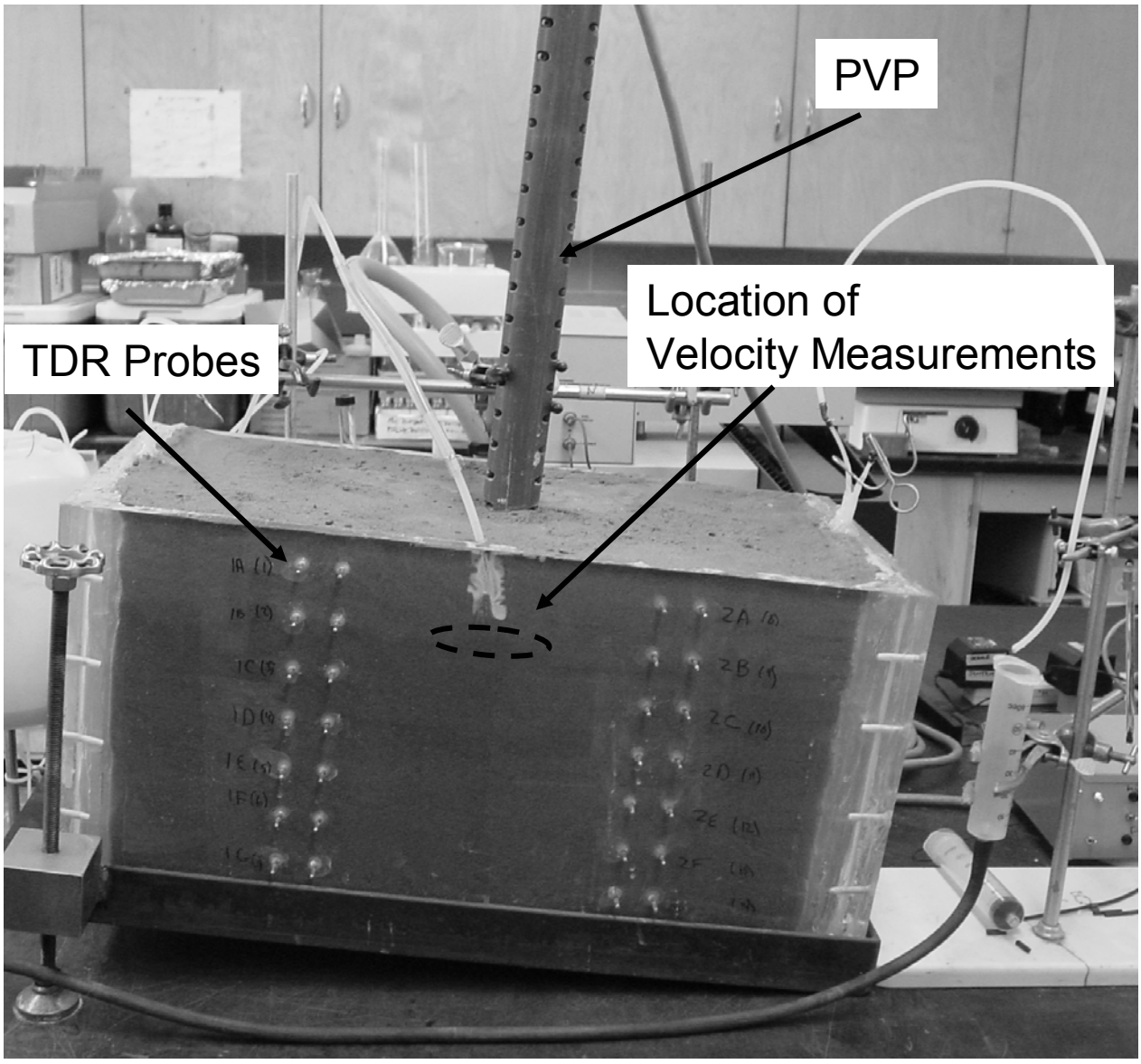

Figure 5.3 Laboratory setup.

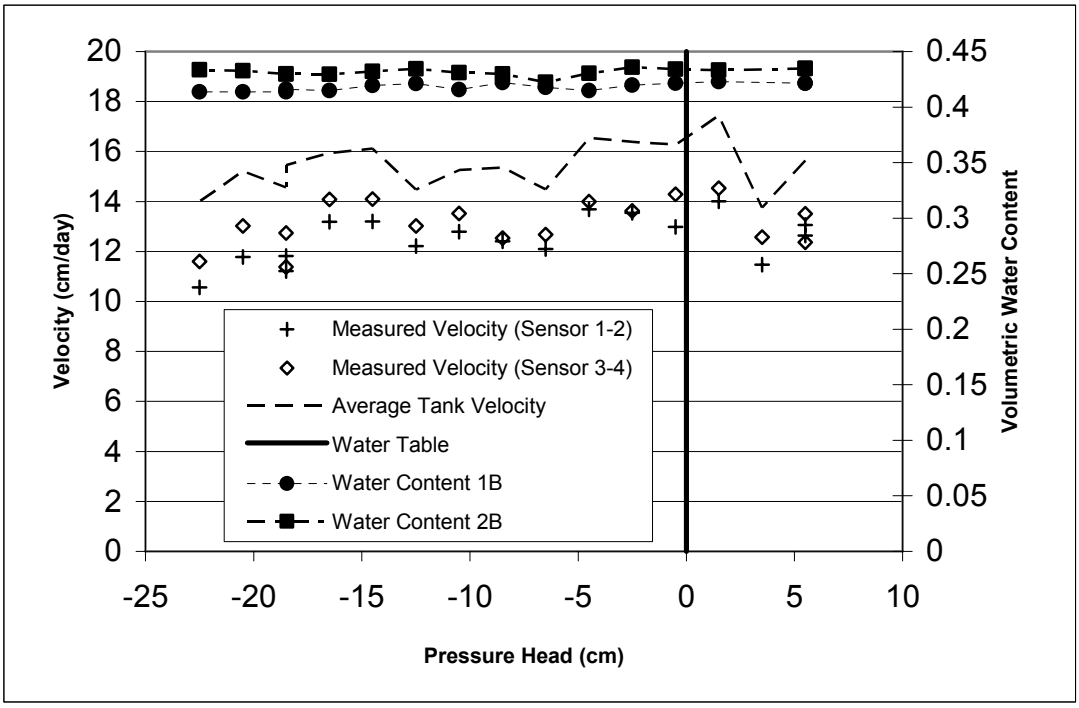

Figure 5.4. 40 μm Experiment – Velocity and water content vs. pressure head.

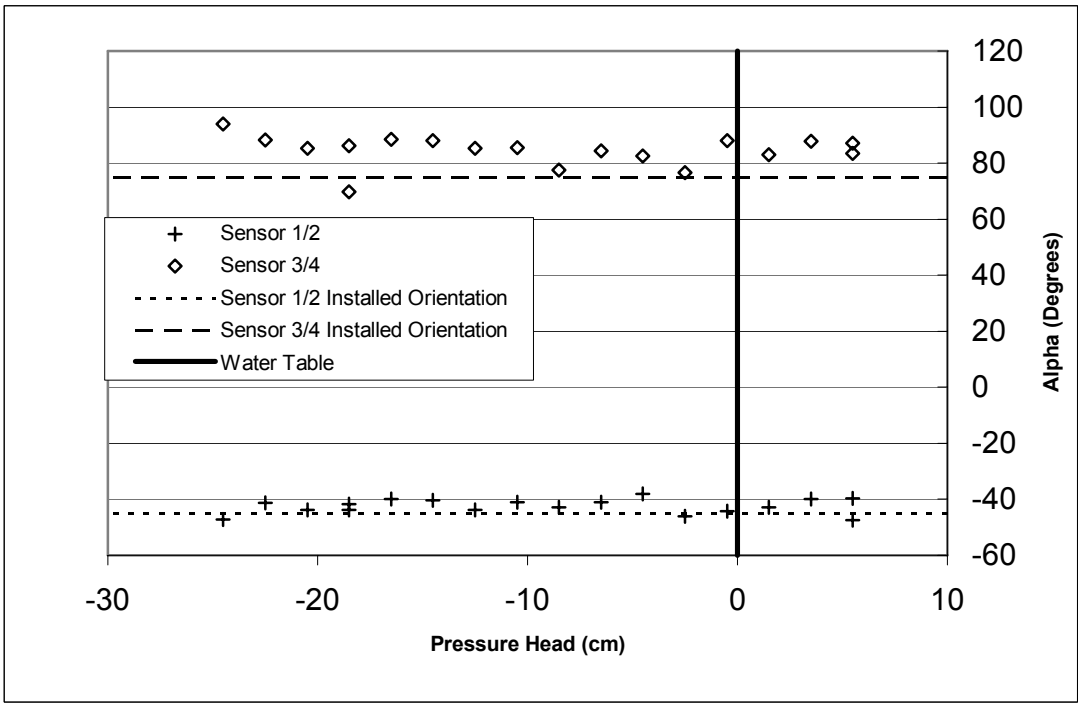

Figure 5.5. 40 μm Experiment – Measured orientation vs. pressure head.

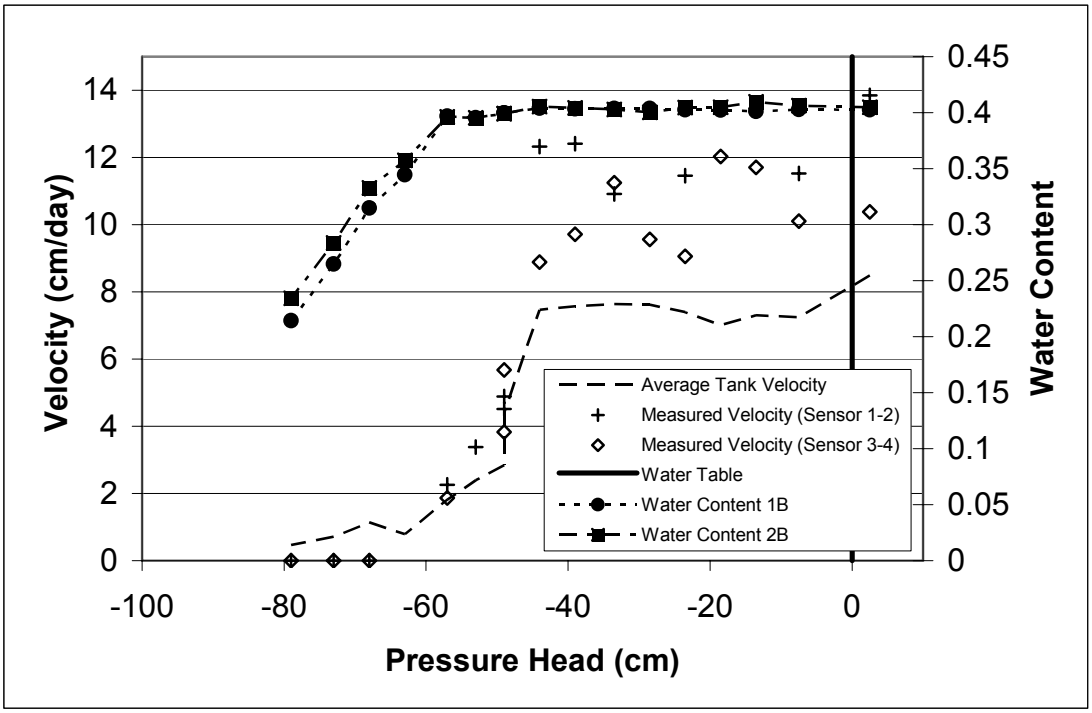

Figure 5.6. 5 μm Drainage Experiment – Velocity and water content vs. pressure head.

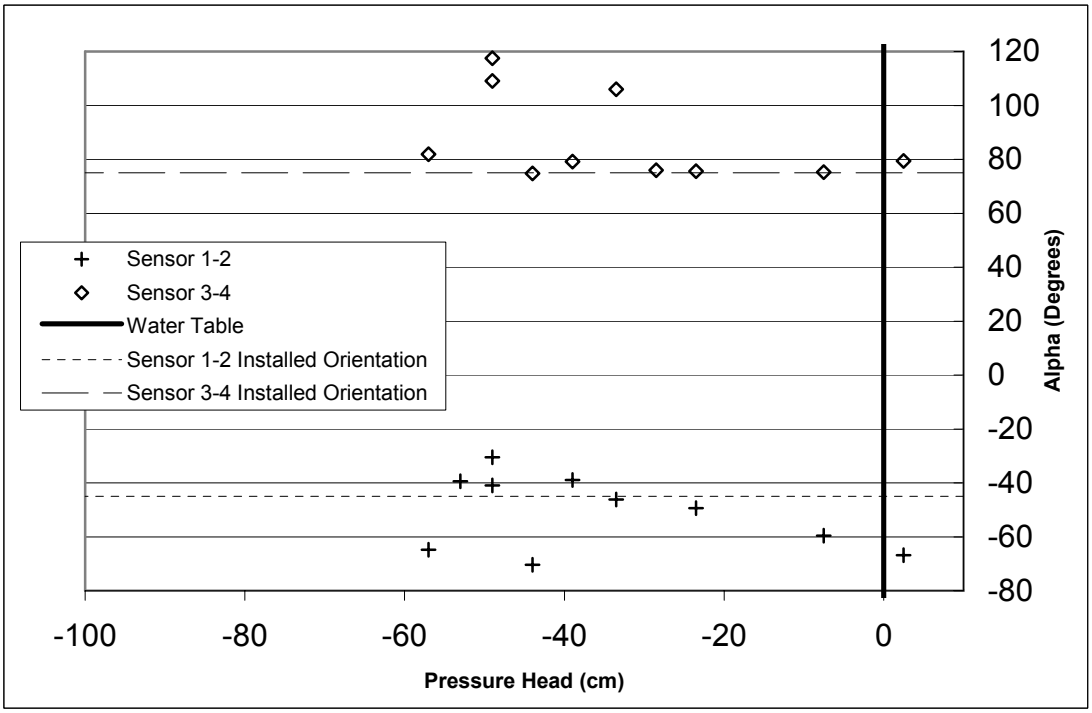

Figure 5.7. 5 μm Drainage Experiment – Measured orientation vs. pressure head.

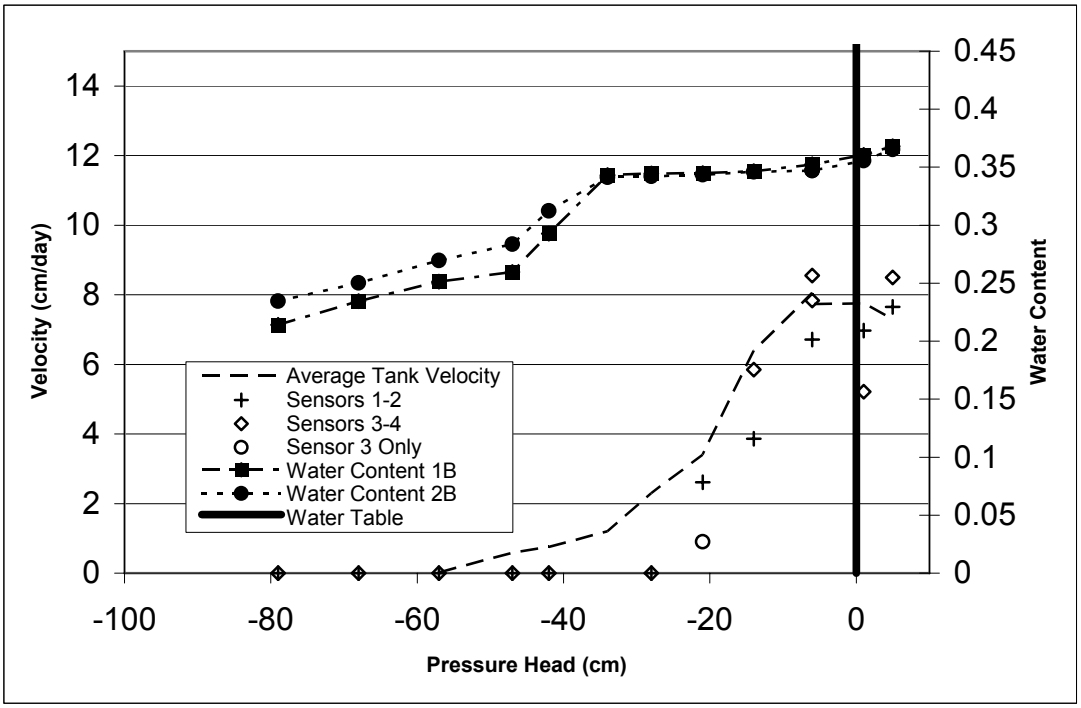

Figure 5.8 5 µm Wetting Experiment – Velocity and water content vs. pressure head.

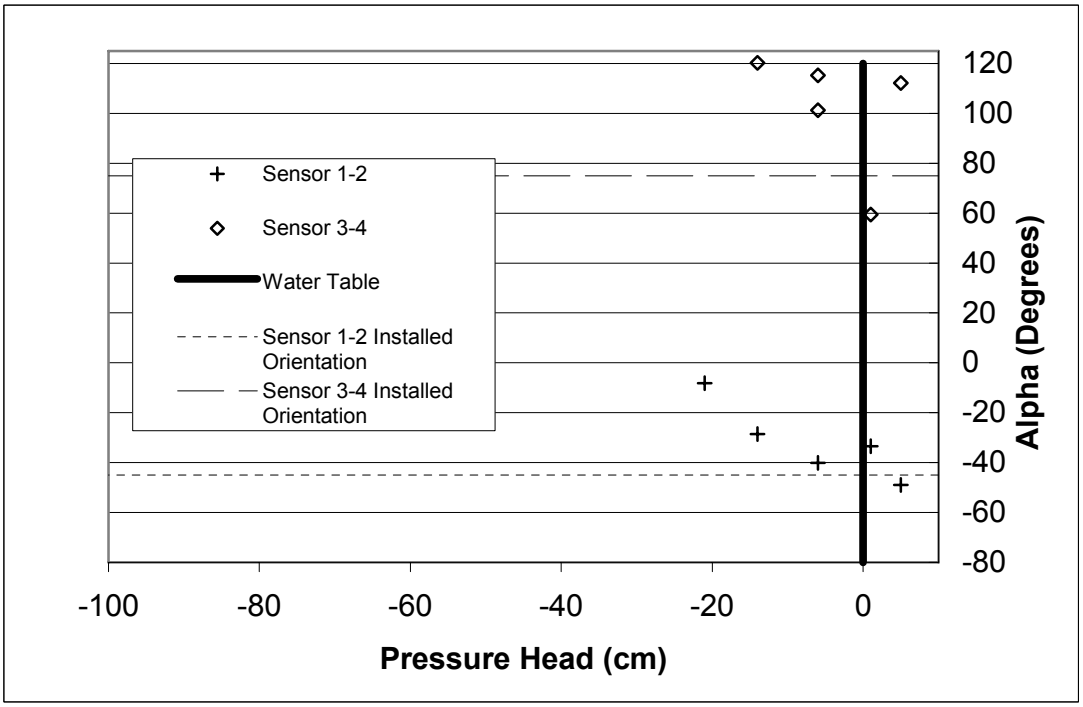

Figure 5.9 5 µm Wetting Experiment – Measured orientation vs. pressure head.

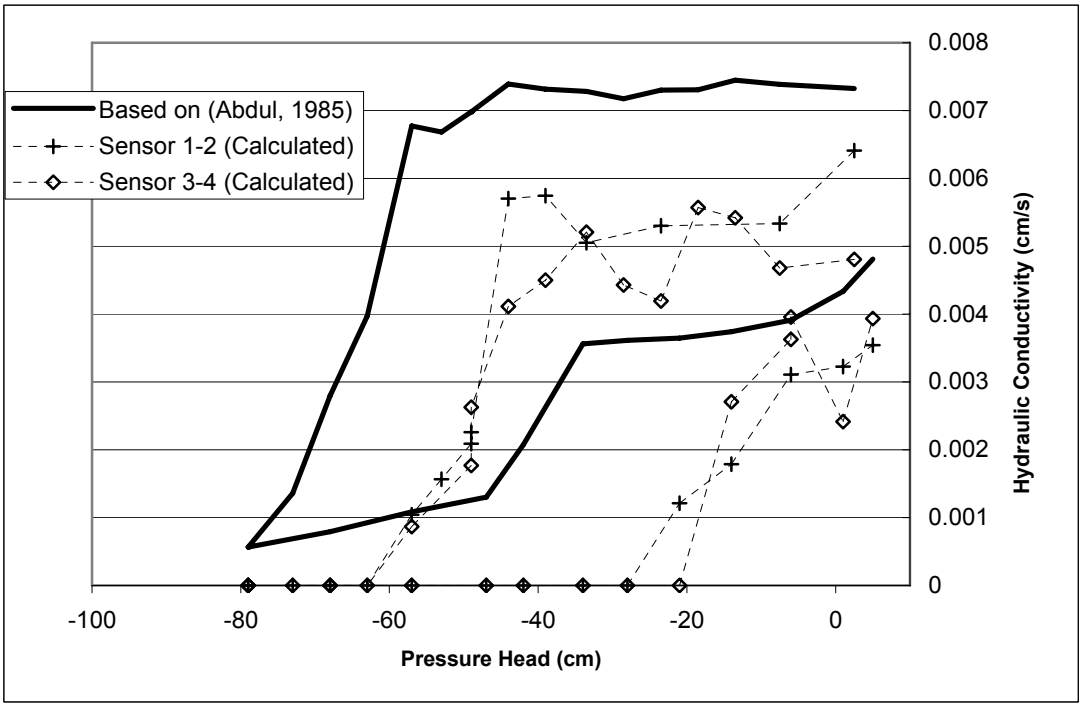

Figure 5.10 5 μm Experiment – Comparison of calculated hydraulic conductivity to measured velocity data.

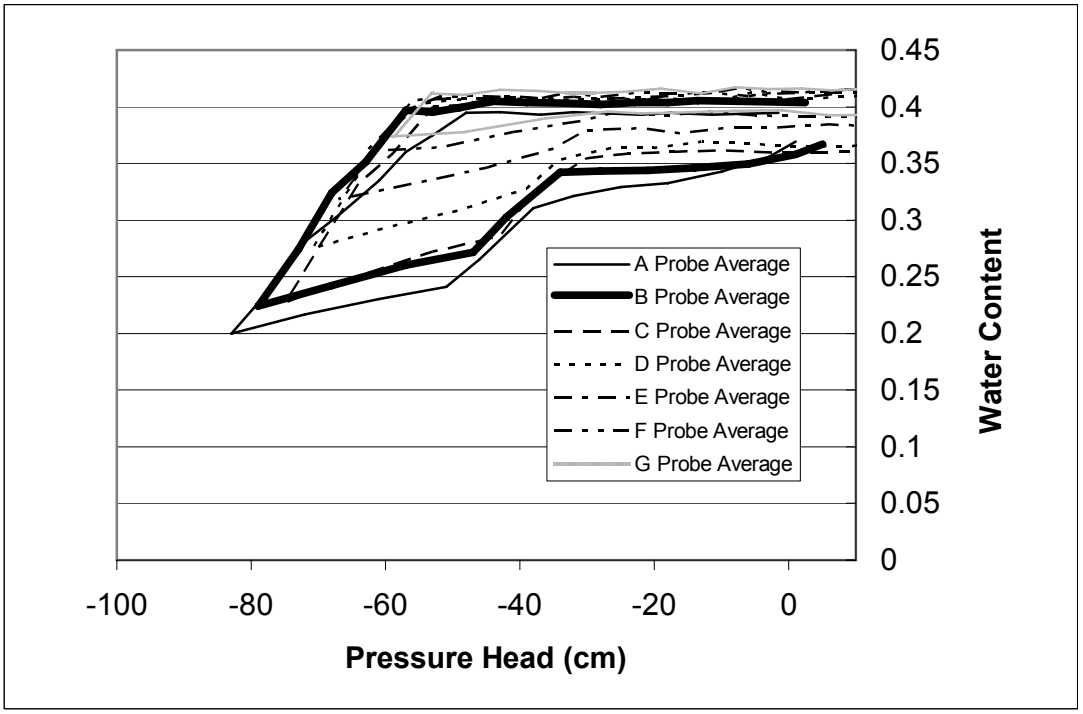

Figure 5.11 5 μm Experiment – Scanning Curves

6. Conclusions and Recommendations

6.1 Conclusions

The goals of this research were to redesign the previous PVP to increase its operational efficiency and to demonstrate the ability of the redesigned PVP to measure groundwater velocity in the capillary fringe. These goals were pursued by modifying the PVP so that it could be operated remotely, and then using the redesigned PVP to investigate groundwater velocity in the capillary fringe under both field and laboratory conditions. The following conclusions are drawn.

1. Changes to the PVP design increased the rate and reliability of data collection. Major design changes include computer controlled motor driven injections, additional sensors and injection ports to allow the probe to be installed without prior knowledge of groundwater flow direction, modification to the way electrical conductivity values are monitored and recorded allow multiple sensors to be recorded over the duration of the test, and the addition of a computer controlled winch to allow for the collection of vertical groundwater velocity profiles.
2. Adapting the PVP system to operate remotely allowed for more efficient data collection while reducing site visits to once a week. If site visits had not been necessary to monitor the flow rate in the controlled flow cell and collect water levels, it would have been possible to run the PVP system remotely for periods greater than one week. This represents cost savings by minimizing the number of hours an operator is required to be onsite while also increasing the rate of data collection.
3. The PVP design is capable of measuring groundwater velocity in the lower portions of the capillary fringe under field conditions (up to 12 cm above the water table). It is suspected that the installation method limits the ability of the probe to measure groundwater velocity in the upper portions of the capillary fringe.
4. Under laboratory conditions, when the probe was in direct contact with the aquifer material it was able to measure groundwater velocity up to 57 cm above the water table.

Thus the limitation of the probe to measure groundwater velocity in the upper portions of the capillary fringe in the field is likely a result of the probe not being in direct contact with the surrounding aquifer material.

5. Groundwater velocity over most of the thickness of the capillary fringe is of a similar magnitude and direction to groundwater velocity below the water table under conditions of drainage.
6. Groundwater velocity in the capillary fringe under wetting conditions appears to be limited due to reduced capillary fringe thickness and the presence of entrapped air.

6.2 Recommendations

1. Increase the volume of the syringes used for injections to allow more groundwater velocity readings to be collected between fillings.
2. Modify the system to increase its portability. A simplification of the electronics and a redesigned extraction system would allow for the entire system to be much more portable for field application.
3. Development of an inexpensive, reliable method for conducting injections that does not require the probe to be extracted to be refilled. This may require the use of a different tracer.
4. Redesign the probe so that it can measure flow in the capillary fringe by expanding (packer set-up) to insure contact with the surrounding soil.
5. Incorporate pressure transducers/tensiometers to determine the location of the probe relative to the water table, eliminating the need for adjacent wells to determine the location of the water table.
6. Addition of vertical velocity sensors located immediately above and below the injection ports to investigate vertical flow under recharge conditions.
7. Investigate the possibility of pouring water down the annular space between the probe and the soil to relieve the tension (reduce the capillary cohesion) and thus promote collapse of the soil around the probe.

8. Install 3 additional sensors, to increase the total to 9 (3 per injection port). See Figure 6.1. This would allow for the measured velocity difference noticed between sensor pair 1-2 and 3-4 to be investigated by comparing values calculated using the first two sensor pairs and values calculated using the second two sensor pairs.
9. Investigate ability of the probe to measure velocity in soils other than sand either through field or laboratory experiments.

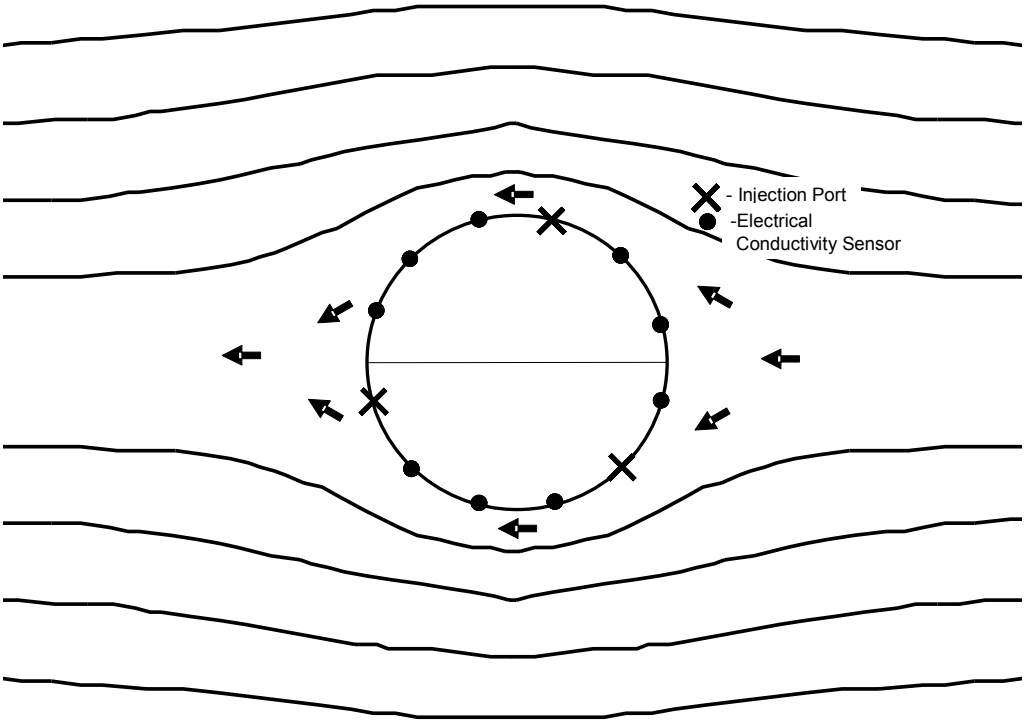

Figure 6.1 Schematic showing position of additional electrical conductivity sensors.

References

Abdul, A. S., Experimental and numerical studies of the effect of the capillary fringe on streamflow generation, Ph. D. University of Waterloo, 1985.

Berkowitz, B., S. E. Silliman and A. M. Dunn, Impact of the Capillary Fringe on Local Flow, Chemical Migration, and Microbiology, *Vadose Zone J, 3*(2), 534-548, 2004.

Bird, R. B., W. E. Stewart and E. N. Lightfoot, Transport Phenomena, John Wiley & Sons, Inc., Toronto, 2002.

Brooks, R. H. and A. T. Corey. Hydraulic properties of porous media. 3. 1964. Fort Collins, Colo., Colorado State University. Hydrology Paper.

Brown, M. J., M. L. McMaster, S. M. Froud, D. J. Katic and J. F. Barker. Passive and semi-passive techniques for groundwater remediation: Phase 1 installation report. 1997. University of Waterloo.

Davies, J. T. and E. K. Rideal, Interfacial Phenomena, Academic, San Diego, Calif., 1963.

Devlin, J. F., A simple and powerful method of parameter estimation using simplex optimization, *Ground Water, 32*(2), 323-327, 1994.

Devlin, J.F., The future of hydrogeology lies in something old something new something borrowed and something else, *Geological Society of America. 36 (5),* 26, 2004.

Di Biase, S. M., An experimental method in groundwater flow measurement: the development of a groundwater velocity probe, University of Waterloo, Waterloo, Ontario, Canada, 1999.

Donald, N. M. An analysis of a poly vinyl chloride groundwater velocity probe. -24. 2001. Waterloo, University of Waterloo. Coop Project Report.

Dunn, A. M. and S. E. Silliman, Air and water entrapment in the vicinity of the water table, *Ground Water, 41*(6), 729-734, 2003.

Fetter, C. W., Applied Hydrogeology Fourth Edition, Prentice Hall, New Jersey, 2001.

Fredlund, D. G. and H. Rahardjo, Soil Mechanics For Unsaturated Soil, John Wiley & Sons, Inc., 1993.

Henry, E. J. and J. E. Smith, Surfactant induced flow phenomena in the vadose zone: a review of data and numerical modeling, *Vadose Zone J, 2*, 154-167, 2003.

Kearl, P. M., Observations of particle movement in a monitoring well using the colloidal borescope, *Journal of Hydrology, 200*, 323-344, 1997.

Kerfoot, W. B., Monitoring well screen influences on direct flowmeter measurements., *Groundwater Monitoring Review Fall,* 74-77, 1985.

Knight, J. H., Sensitivity of time domain reflectometry measurements to lateral variations in soil water content, *Water Resources Research, 28*(9), 2345-2352, 1992.

Labaky, W., Theory and testing of a device for measuring point-scale groundwater velocities, Ph. D. University of Waterloo, 2004.

Lapham, W. W., F. D. Wilde and M. T. Koterba. Guidelines and standard procedures for studies of ground-water quality: Selection and installation of wells, and supporting documentation. 96-4233, 1-110. 1997.

Luthin, J. N. and P. R. Day, Lateral flow above a sloping water table, *Soil Science Society Proceedings, 19*, 406-410, 1955.

MacFarlane, D. S., J. A. Cherry, R. W. Gillham and E. A. Sudicky, Migration of contaminants in groundwater at a landfill: A case study. 1. Groundwater flow and plume delineation, *Journal of Hydrology, 63*, 1-29, 1983.

Mackay, D. M., D. L. Freyberg, P. V. Roberts and J. A. Cherry, A natural gradient experiment on solute transport in a sand aquifer, 1. Approach and overview of plume movement, *Water Resources Research, 22*(13), 2017-2029, 1986.

McGlashan, M. A., G. P. Tsoflias, P. C. Schillig and J. F. Devlin, Estimating groundwater flow velocity using borehole GPR and point velocity probes, 2006.

Molson, J. W. and E. O. Frind. SALTFLOW Version 3.0 Density-Dependent Flow and Mass Transport Model in Tree Dimensions, User Guide. -67p. 2002. University of Waterloo, Waterloo.

Mualem, Y., Hysteretical models for prediction of the hydraulic conductivity of unsaturated porous media, *Water Resources Research, 12*(6), 1248-1254, 1976.

Nwankwor, G. I., J. A. Cherry and R. W. Gillham, A Comparative-Study of Specific Yield Determinations for A Shallow Sand Aquifer, *Ground Water, 22*(6), 764-772, 1984.

Or, D., S. B. Jones, J. R. VanShaar, S. Humphries and L. Koberstein. WinTDR soil analysis software. 2003. Utah State University.

Ronen, D., B. Berkowitz and M. Margaritz, The development and influence of gas bubbles in phreatic aquifers under natural flow conditions, *Transport in Porous Media, 4*, 295-306, 1989.

Ryan, M. C., K. T. B. MacQuarrie, J. Harman and J. McLellan, Field and modeling evidence for a "stagnant flow" zone in the upper meter of sandy phreatic aquifers, *Journal of Hydrology, 233*, 223-240, 2000.

Silliman, S. E., B. Berkowitz, J. Simunek and M. T. van Genuchten, Fluid flow and solute migration within the capillary fringe, *Ground Water, 40*(1), 76-84, 2002.

Smith, J. E. and R. W. Gillham, The effect of concentration-dependent surface tension on the flow of water and transport of dissolved organic compounds: A pressure head-based formulation and numerical model, *Water Resources Research, 30*(2), 343-354, 1994.

Smith, J. E. and R. W. Gillham, Effects of solute concentration-dependent surface tension on unsaturated flow: Laboratory sand column experiments, *Water Resources Research, 35*(4), 973-982, 1999.

Sudicky, E. A., A natural gradient experiment on solute transport in a sand aquifer: spatial variability of hydraulic conductivity and its role in the dispersion process, *Water Resources Research, 22*(13), 2069-2082, 1986.

van Genuchten, M. T., A closed-form equation for predicting the hydraulic conductivity of unsaturated soil, *Soil Science Society of America Journal, 44*, 892-898, 1980.

Wyckoff, R. D., H. G. Botset and M. Muskat, Flow of liquids through porous media under the action of gravity, *Physics, 3*, 90-113, 1932.

Xie, X., Solute transport and remediation in the interface zone: Mathematical modelling and field investigations, Ph. D. University of Waterloo, 1994.